LAMASUS

Land Management for Sustainability

D7.1 Implementation of additional LUM systems and land use dynamics into macro-level models

This project has received funding from the European Union's Horizon Europe Research and Innovation programme under Grant Agreement No 101060423. The information and views set out in this deliverable are those of the author(s) and do not necessarily reflect the official opinion of the European Union. Neither the European Union institutions and bodies nor any person acting on their behalf may be held responsible for the use which may be made of the information contained therein.

Funded by the European Union

Grant Agreement	101060423
Call identifier	HORIZON-CL6-2021-GOVERNANCE-01
Project full title	Land use and management modelling for sustainable governance
Work package	WP 7
Due date	31/05/2026
Deliverable lead	Tamás Krisztin (IIASA)
Authors	Stefan Frank, Leopold Ringwald, Ipsita Kumar, Tamás Krisztin, Michael Wögerer, Omid Zamani, Pekka Lauri and Fanqi Jia (IIASA), Jordan Hristov (EC/IIASA), Elisa Bardazzi, Willem-Jan van Zeist (WUR), Ana-Luisa Barbosa (JRC), Jonathan Doelman (PBL), Peter Witzke, David Schäfer (EC)

Abstract

This deliverable documents how the LAMASUS macro-level models—GLOBIOM, CAPRI, IMAGE and MAGNET—have been extended to represent land-use and land-use management systems explicitly, and to reflect the behaviour observed in historical land-use change. It reports the work carried out under Tasks 7.1 and 7.2 of WP7.

We report four sets of developments. First, the historic land-use and management information of the LUM geodatabase (WP2) is taken up by each model at its highest feasible spatial resolution. Second, the CAP Strategic Plans are encoded intervention by intervention in the CAPRI premium module and passed on to GLOBIOM and MAGNET. Third, organic farming, grassland management, climate-smart forest management and peatland rewetting are introduced as distinct management options with their own yields, costs and emission factors. Fourth, the econometric parameters estimated in WP4 are translated into technical yield shifters and land-use change parameters. Together, these developments allow the models to assess policies that act through differentiated management requirements rather than through aggregate land-use categories, providing the model basis for the scenario work in WP8.

Keywords

Land use modelling, land use management, Common Agricultural Policy, ex-ante policy assessment, macro-level models

Internal Technical Auditor	Name (Beneficiary short name)	Date of approval
Task leader	Tamás Krisztin (IIASA)	28/08/2026
WP leader	Tamás Krisztin (IIASA)	28/08/2026
Coordinator	Petr Havlík (IIASA)	28/08/2026
Project Management Office (PMO)	Ellen Tan (IIASA)	02/09/2026

Dissemination level

PU	Public, will be published on CORDIS	✓
SEN	Sensitive. Confidential information, only for members of the Consortium (including the EC services)	

Nature of the deliverable	*R*

Table of Contents

List of Figures

List of Tables

Abbreviations

AEZ	Agro-ecological zone
ANC	Areas with Natural Constraints
BECCS	Bioenergy with carbon capture and storage
BISS	Basic Income Support for Sustainability
CAPRI	Common Agricultural Policy Regionalized Impact model
CBI	Carbon balance indicator
CIS	Coupled Income Support
CLC	Corine Land Cover
CSF	Climate-smart forestry
CSP	CAP Strategic Plan
DF	Displacement factor
EC	European Commission
ENVCLIM	Environmental, Climate-related and Other Management Commitments
ESA-CCI	European Space Agency Climate Change Initiative
EWM	European Wetland Map
FADN	Farm Accountancy Data Network
FAO	Food and Agriculture Organization of the United Nations
FRA	Global Forest Resources Assessment
FSS	Farm Structure Survey
G4M	Global Forest Model
GAEC	Good Agricultural and Environmental Conditions
GHG	Greenhouse gas
GLOBIOM	Global Biosphere Management Model
GRAE	Extensive grassland
GRAI	Intensive grassland
HWP	Harvested wood products
HYDE	History Database of the Global Environment
IMAGE	Integrated Model to Assess the Global Environment

IPCC	Intergovernmental Panel on Climate Change
JRC	Joint Research Centre (European Commission)
LUM	Land use and management
MAGNET	Modular Applied GeNeral Equilibrium Tool
MNL	Multinomial logit
NUTS	Nomenclature of Territorial Units for Statistics
PUA	Planned unit amount
RGDPPC	Real gross domestic product per capita
SimU	Simulation Unit
SSP	Shared Socioeconomic Pathway
UNFCCC	United Nations Framework Convention on Climate Change
WP	Work Package

Executive summary

The LAMASUS project develops an integrated modelling toolbox to support the policy needs of the European Green Deal. Its macro-level models—GLOBIOM, CAPRI, IMAGE and MAGNET—are widely used for EU policy assessment, but their traditional representations rely on stylised production systems, limited differentiation of land management practices, and behavioural responses that are implicitly calibrated. As EU policy increasingly targets specific management practices rather than aggregate land-use outcomes, this limits the policy questions the models can answer.

The LAMASUS project addresses these limitations by extending the macro-level models. This deliverable documents the work carried out under Tasks 7.1 and 7.2 of work package (WP) 7 and covers four sets of developments:

First, the historic land-use and management information of the LUM geodatabase developed in WP2 is taken up by each model at its highest feasible spatial resolution. GLOBIOM re-derives its baseline land-use and crop distributions from the geodatabase, CAPRI uses it to replace the previous 50:50 grassland intensity assumption with regionally differentiated shares, and IMAGE/MAGNET uses it to validate its global land-use/cover dataset for Europe.

Second, each model encoded European policy instruments. The CAPRI premium module reads the CAP Strategic Plans intervention by intervention and links agri-environmental payments to endogenous farm practices, GLOBIOM takes over the resulting payment rates and budget ceilings, and MAGNET represents the CAP through Pillar 1 and Pillar 2 subsidy categories with econometrically parameterised productivity effects.

Third, we expanded the set of management systems explicitly represented. Organic farming and grassland management become distinct production options in CAPRI and GLOBIOM, with their own yields, costs, emission factors and market premiums. Climate-smart forest management systems are implemented in G4M, alongside a more detailed representation of harvested wood products, substitution effects and the forestry sector in MAGNET. Furthermore, peatland rewetting is represented as a distinct mitigation option in CAPRI, GLOBIOM and IMAGE, based on spatially explicit peatland maps.

Fourth, the econometric parameters estimated in WP4 are translated into model inputs—technical yield shifters derived from a multilevel Bayesian panel model and projected under the Shared Socioeconomic Pathways, and land-use change parameters estimated from observed European land-cover transitions.

Together, these developments allow the macro-level models to assess policies that act through differentiated management requirements rather than through aggregate land-use categories, and to do so within behavioural limits derived from observed land-use change. The

models documented here are the direct input to the baseline and scenario work of WP8, where the policy scenarios that use them are simulated and analysed (forthcoming in D8.1, D8.2).

1. Introduction

Land-use and land-use management choices are central to Europe's climate, biodiversity, and agricultural policy agenda. Decisions on how land is managed—through farming systems, grassland intensity, forest management regimes, or the treatment of peatlands—simultaneously shape greenhouse gas (GHG) emissions, carbon sequestration, ecosystem services, and rural incomes. As EU policy instruments increasingly target specific land management practices rather than aggregate land-use outcomes, policy analysis requires macro-level economic models that can represent management systems and behavioural constraints with greater realism than has been customary.

Ex-ante macro-level models such as CAPRI, GLOBIOM, and MAGNET/IMAGE are widely used for EU policy assessment and have played a critical role in analysing agricultural, climate, and land-use policies. These models capture market-mediated responses, trade effects, and cross-sectoral interactions that are essential for forward-looking analysis. However, their traditional representations rely on stylised production systems, limited differentiation of land management practices, and behavioural responses that are often calibrated implicitly or represented at highly aggregated spatial scales. While sufficient for broad scenario exploration, these features limit the models' ability to assess policies that operate through differentiated management options, adjustment frictions, and spatially heterogeneous constraints.

The LAMASUS project addresses these limitations by strengthening the empirical and behavioural foundations of macro-level land-use models, drawing on the spatial, environmental, and econometric evidence developed elsewhere in the project, while preserving their capacity for consistent EU-wide and global analysis. Within this framework, Work Package 7 focuses on upgrading the internal structure of the macro-level models so that they can systematically incorporate this evidence. This deliverable, D7.1, documents these upgrades and explains how they extend the state of the art in policy-relevant land-use modelling.

This report covers the implementation of Tasks 7.1 and 7.2. Its objective is to document how macro-level models have been modified to better represent land-use management systems and local land-use dynamics, in a way that is empirically grounded, transparent, and suitable for ex-ante policy analysis. For an overview on where the deliverable fits into the project, see Figure 1.

Task 7.1 focuses on improving the explicit representation of land-use and management systems in macro-level models. Building on spatially explicit land-use and management data, as well as environmental and economic indicators developed earlier in the project, the models are extended to distinguish management options that are directly relevant for climate mitigation, biodiversity protection, and agricultural policy. These extensions are implemented in a way that is consistent with each model's structure and policy use, while relying on harmonised assumptions wherever possible.

Task 7.2 addresses a complementary challenge: the weak representation of local behavioural dynamics in macro-level projections. Land-use change is constrained by adjustment costs, institutional frictions, and historically observed response patterns. To reflect these constraints, behavioural parameters estimated in econometric analyses are integrated into the macro-level models at the highest feasible spatial resolution. This strengthens the link between observed land-use dynamics and forward-looking scenario projections.

Together, Tasks 7.1 and 7.2 aim to ensure that macro-level models respond to policy signals not only through prices and rents, but also through realistic management choices and empirically grounded limits to change.

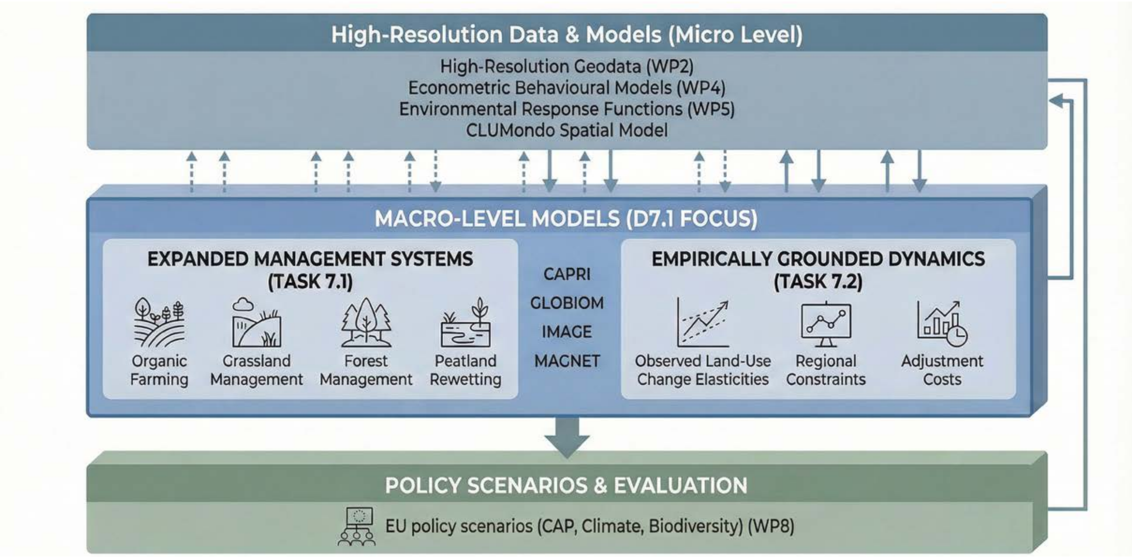

Figure 1: Overview of D7.1 and its role in LAMASUS

A central contribution of this deliverable is to enhance detailed management system information within macro-level models. Rather than treating land-use categories as homogeneous, the models now differentiate management regimes with distinct productivity, cost, and environmental profiles.

In CAPRI and GLOBIOM, organic farming and grassland management are represented explicitly. Organic farming is implemented as a distinct production option with empirically grounded yield differences, cost structures, emission factors, and market premiums. This allows the models to capture both supply-side constraints and demand-driven incentives associated with organic production. Grassland systems are differentiated by management intensity, enabling analysis of extensification, grazing pressure, and silvopastoral practices in a manner consistent with CAP instruments and climate objectives.

In MAGNET, the economic representation of forestry is expanded with a more detailed representation of harvested wood products and a separate paper & pulp sector, and with mechanisms that align the dynamic competition between forestry and agricultural land uses with GLOBIOM. These extensions improve the models' ability to capture land competition and long-term land allocation effects under climate and energy policies. Within GLOBIOM, the forest sector model G4M is further developed to represent climate-smart forest management regimes, capturing alternative harvesting strategies and their implications for carbon stocks and timber supply.

Across all three macro-level models, peatland rewetting is implemented or refined as a distinct climate mitigation option. This representation relies on spatially explicit peatland maps and mitigation potentials, and accounts for both emission reductions and opportunity costs. By moving beyond aggregate emission factors, the models can assess peatland policies alongside other land-use and management measures within a consistent economic framework.

While improved management system detail is necessary, it is not sufficient to generate realistic land-use projections. Macro-level models must also reflect the behavioural limits observed in historical land-use change. Task 7.2 addresses this requirement by integrating econometric parameters into the modelling frameworks.

Historic land-use and management information is first incorporated at the highest feasible spatial resolution in each model. Building on this baseline, behavioural parameters estimated in econometric analyses—such as elasticities of land-use change or constraints on adjustment speed—are translated into model-specific parameters.

For CAPRI and MAGNET, this primarily takes the form of land-use and management elasticities that govern the responsiveness of land allocation to economic signals. For GLOBIOM, a broader set of behavioural parameters is implemented, including constraints on maximum and minimum land-use change at the regional level and additional cost terms reflecting adjustment frictions. These implementations preserve structural differences between models while embedding a common behavioural logic derived from observed land-use dynamics. In addition, the downscaling routines developed in WP7 (Section 5.2) translate macro-level land-use results back to the grid level, using the same econometrically estimated land-use change parameters, thereby closing the loop between the macro-level models and the observed local dynamics.

The modifications documented in this deliverable go beyond incremental model refinement. By combining explicit representation of land-use management systems with empirically grounded behavioural constraints, the macro-level models move closer to observed land-use dynamics while retaining their ability to assess long-term policy scenarios consistently.

These advances are particularly relevant for EU policies that rely on differentiated incentives, conditionalities, and restoration targets. They also provide a stronger foundation for the integrated scenario analysis conducted later in the project (to be documented in D8.2), where macro-level economic responses must be translated into credible land-use and management outcomes across regions.

The remainder of this report is structured as follows. Section 2 describes the uptake of historic land-use and management information into the macro-level models. Sections 3 and 4 present the improved representation of European policies and land-use management systems, respectively. Section 5 details the integration of behavioural parameters. The report concludes by outlining how these advances support subsequent policy analysis.

2. Uptake of historic information from the LUM geodatabase

The purpose of this chapter is to document, per model, the first step of Task 7.2: the uptake of historic land-use and management information from the LUM geodatabase at each model's highest feasible resolution. The extent of uptake differs across models, reflecting their native spatial resolution and data architecture. GLOBIOM, which operates on a high-resolution simulation grid, re-derives its baseline land-use and crop distributions directly from the geodatabase. IMAGE/MAGNET incorporates the geodatabase into its global land-use/cover dataset (at least national level) and validates it against the existing representation. CAPRI, which operates at the NUTS2 level, draws on the geodatabase for targeted refinements — notably grassland management — while retaining its established statistical sources for consistency. For each model, the sections below describe which information is taken up, at which spatial resolution, and what is deferred to later work.

2.1. UPTAKE IN CAPRI

In CAPRI, land use is represented through a multi-source data consolidation process. Raw land-use data are drawn from several complementary sources, including Eurostat's national and regional land-use statistics (REGIO, LANDCOVER), Corine Land Cover (CLC) data transformed via LUCAS contingency tables, FAOSTAT, the harmonised EU-wide land-use change dataset HILDA+ (Winkler et al., 2021), the EU Farm Structure Survey (FSS), and UNFCCC Common Reporting Format data on land-use transitions for LULUCF accounting. CAPRI therefore already shares part of its empirical basis with the LUM geodatabase, which likewise builds on the CORINE land-cover layers, Eurostat, and FAO.

The most direct uptake of the LUM geodatabase in CAPRI concerns grassland management. As detailed in Section 4.3.2, the geodatabase is used to refine the split between extensive and intensive grassland, replacing the previous 50:50 assumption with regionally differentiated shares.

Beyond this targeted refinement, the geodatabase has not been taken up for the spatial allocation of cropland. CAPRI operates at NUTS2 rather than on a grid, and its area data are kept aligned with the Eurostat yield and production statistics the model already uses, ensuring coherent area, yield and production figures for cropland.

2.2. UPTAKE IN GLOBIOM

This section describes the uptake of the spatially explicit Land Use and Management (LUM) geodatabase developed in WP2 into the GLOBIOM modelling framework. The objective is to harmonise GLOBIOM's land and crop supply representation with the high-resolution, observation-based geodatabase, improving the spatial realism of the baseline land-use and crop distributions used in model simulations. The integration follows a three-step workflow: (i) the crops represented in GLOBIOM are distributed over the LUM cropland using a probability-based allocation; (ii) the resulting crop-specific layers are combined with the remaining LUM land-cover classes and aggregated to GLOBIOM's Simulation Unit (SimU) grid; and (iii) the aggregated layers are used to update GLOBIOM's base input data, yielding a baseline that is fully consistent with the LUM geodatabase. The three steps are described in Figure 2 and illustrated for Austria.

In the first step, the crops represented in GLOBIOM are distributed across the cropland identified in the LUM geodatabase. Only areas classified as arable cropland are eligible for allocation; all other land-cover classes are excluded, so that crop allocation is fully constrained by observed land-use patterns. Within the eligible cropland, crop-specific allocation probabilities are derived from the priors of Baumert et al. (2024), which combine biophysical suitability, historical land-use patterns, and agronomic constraints to favour locations where cultivation is agronomically plausible. The allocation is then scaled iteratively so that the area of each crop matches the corresponding GLOBIOM baseline target at the regional level, preserving the model's aggregate crop areas and supply calibration. Cropland left unallocated after all represented crops have been assigned is retained as residual cropland and labelled as 'Other natural land', consistent with GLOBIOM's land-use accounting.

In the second step, the crop-specific cropland layers are combined with the remaining LUM land-cover classes and aggregated from the native geodatabase resolution to GLOBIOM's Simulation Unit (SimU) grid — the highest resolution at which the model operates. Aggregation uses area-weighted summation, so that the fractional land-cover composition of each SimU cell reflects the underlying high-resolution data while preserving observed spatial heterogeneity.

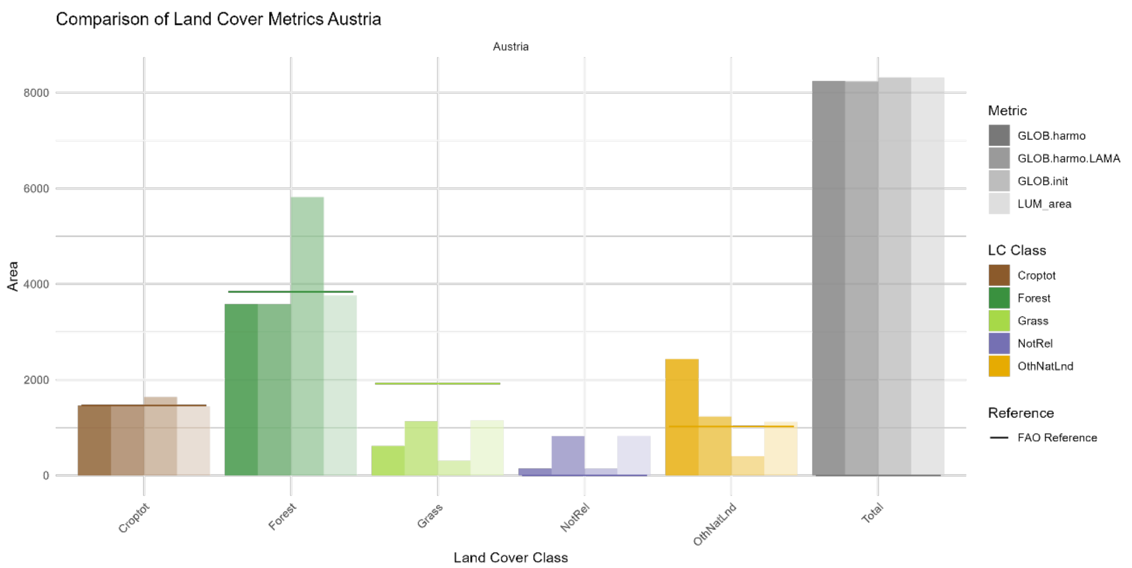

Figure 2: Comparison of land-cover metrics for Austria, in 1000 ha.

Note: Land-cover classes: Croptot (total cropland), Forest, Grass (grassland), NotRel (classes not represented in GLOBIOM), OthNatLnd (other natural land). Metrics: GLOB.init — original GLOBIOM baseline input; GLOB.harmo and GLOB.harmo.LAMA — GLOBIOM inputs harmonised with the LUM geodatabase, before and after the trade and supply–demand calibration adjustment; LUM_area — area according to the LUM geodatabase. Horizontal lines give the FAO reference value per class.

In the final step, the aggregated SimU-level land-use and crop layers are used to update GLOBIOM's base input data, replacing the original baseline layers for land availability, crop areas, and initial supply conditions. The model baseline thereby becomes fully harmonised with the LUM geodatabase, so that subsequent scenario simulations start from a land-use configuration that reflects observed patterns rather than stylised distributions. Figure 2 compares, for Austria, the updated GLOBIOM inputs with the original inputs (GLOB.init), before and after the trade and supply–demand calibration adjustment.

2.3. UPTAKE IN IMAGE/MAGNET

The land-use information in IMAGE and MAGNET is based on a global land-use/cover dataset specifically developed for these models, using a range of data sources. To assess the feasibility and implications of replacing the default IMAGE/MAGNET land-use/cover data with the LUM geodatabase for Europe, we conducted a detailed comparison of the two datasets at the EU Member State and NUTS2 levels.

The IMAGE/MAGNET global land-use/cover database

Based on a number of data sources, a consistent land-use/cover map with eight categories was created: 1) built-up area; 2) cropland, 3) managed grazing land; 4) other anthropogenic land; 5) managed forest; 6) natural forest; 7) other natural land; and 8) ice (Figure 3), with fractional detail at a spatial resolution of 5 arc-minutes.

The basis is the ESA-CCI land-cover dataset (spatial resolution: 10 arc-seconds; Hollmann et al., 2013), which was converted into six broad land-cover categories (i.e., cropland, grassland, forest, other natural land, built-up area, and ice) (see SI Table 1) at a resolution of 5 arc-minutes. Water is excluded from the analysis.

Grassland is further divided into anthropogenic and natural grassland. Grassland is classified as anthropogenic if it is located in natural forest biomes (according to IUCN) and where population density exceeds 0.1 person per km^2 (Klein Goldewijk et al., 2010), under the assumption that such grasslands have been actively converted by humans.

The ESA-CCI built-up area is replaced with results from the 2UP model (van Huijstee et al., 2018). For the historical period, 2UP is based on Global Human Settlement Layer (GHSL) data (Schiavina et al., 2023), while for the scenario period, built-up area is determined by population projections and other assumptions.

Cropland and managed grassland data from ESA-CCI are replaced with data from the HYDE database (Klein Goldewijk et al., 2017) which is consistent with FAO statistics. If the combined area of built-up land, cropland, and managed grassland exceeds the total grid cell land area, managed grassland is reduced first, followed by cropland.

Generally, ESA-CCI estimates of cropland and anthropogenic grassland are larger than those from HYDE. The difference typically reflects land that is used anthropogenically, but not recorded in agricultural statistics, as it captured in other use, e.g. local infrastructure, small forest patches or degraded forest, informal agricultural land, or recreational areas. These areas are classified as a separate category called 'other anthropogenic land.' This category is calculated as the difference between ESA-CCI cropland and anthropogenic grassland and the corresponding HYDE cropland and grassland, calculated at 5 arc-minute resolution. If HYDE cropland and grassland exceed ESA-CCI cropland and anthropogenic grassland values, 'other anthropogenic land' is set to zero by definition.

The ESA-CCI forest class is split into managed and unmanaged forests using the global forest management layer produced by Lesiv et al. (2022). Forest areas classified as naturally regenerating with signs of management, planted forests and plantation forests are considered managed, while naturally regenerating forests without signs of management are considered unmanaged. For each grid cell, the shares of managed/unmanaged from Lesiv et al. are multiplied by the ESA-CCI forest area, preserving ESA-CCI total forest cover while incorporating management information.

Finally, ESA-CCI classes for other natural land and natural grasslands are combined into a single "other natural land" class, while the ESA-CCI "ice" class is retained unchanged. If the combined area of natural forest, managed forest, other natural land, and ice classes together with the other land-use categories exceeds the grid cell area, the newly created four classes are scaled down to ensure that the total does not exceed the available land area.

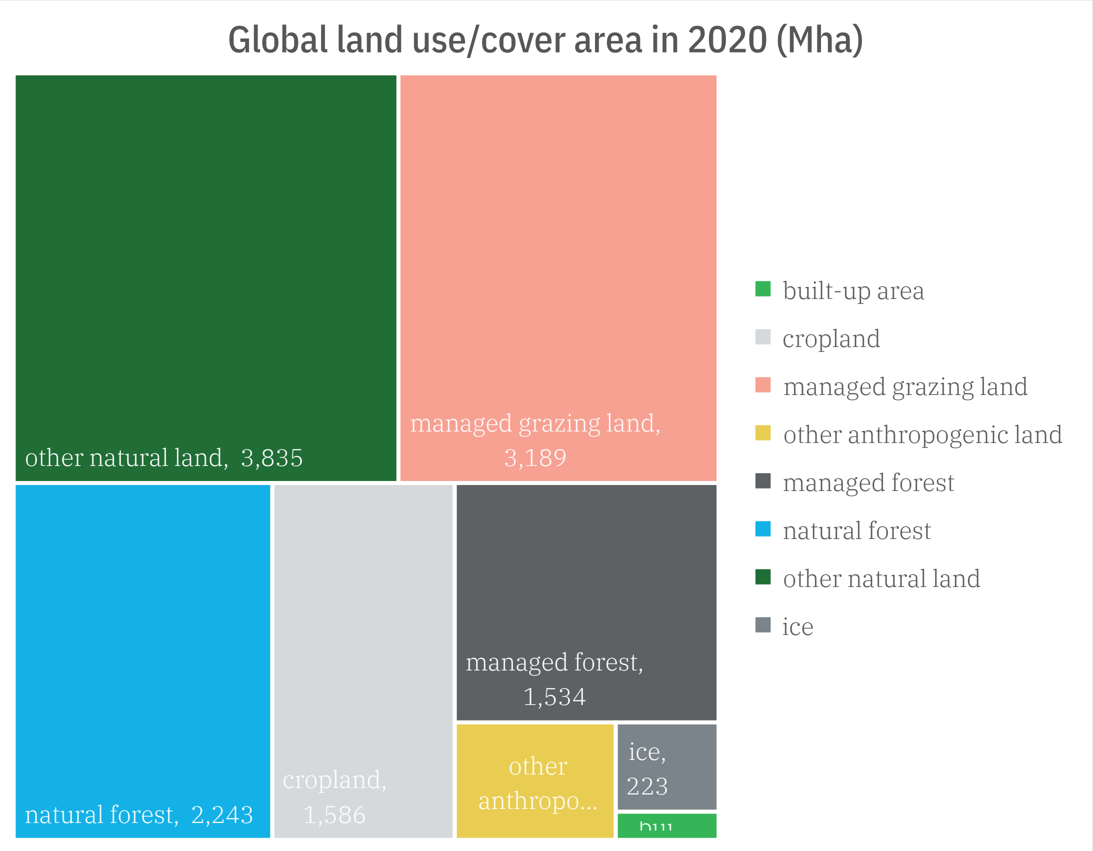

Figure 3: Total area per land-use/cover category for 2020 (in Mha) from IMAGE/MAGNET's global land-use/cover dataset

Note: Values in total area in Mha (as a percent of total) per land-use category: Other natural land: 3,835 Mha (29.2%), managed grazing land: 3,189 Mha (24.3%), natural forest: 2,243 Mha (17.1%), cropland:

1,586 Mha (12.1%), managed forest: 1,534 Mha (11.7%), other anthropogenic land: 460 (3.5%), ice 223 Mha (1.7%), and built-up area 70 Mha (0.5%).

Comparing the LUM database with the IMAGE/MAGNET land-use/cover dataset

A comparison between the LUM database and the IMAGE/MAGNET land-use/cover dataset (from now on referred to as IMAGE) was made by mapping all LUM database categories to the coarser IMAGE land-use/cover categories (see Annex Table *12*).

Total area aligns well between the two datasets for most countries. The least-squares linear regression analysis at the NUTS2 level provides an R^2 of 1.00, confirming the agreement (Figure 4). For Finland and Sweden, IMAGE is quite a bit lower than the LUM database, which may be related to differences between how the underlying ESA-CCI and Corine land cover datasets detect water bodies.

For cropland, the datasets are reasonably well aligned (R^2=0.96), but less so than for total area. For IMAGE, cropland area relies on FAOSTAT as processed for the HYDE database, while the LUM database relies on Eurostat. The variation therefore may arise from differences in the underlying regional data sources or how HYDE allocates cropland areas to the NUTS2 level.

The managed grazing land category does not have great agreement between IMAGE and LUM at the NUTS2 level (R^2=0.77), while at the EU level the difference is not so large, with 53 Mha in IMAGE and 47 Mha in LUM. At the member-state level there are substantial differences where most countries have larger areas in IMAGE compared to LUM (notably Spain with 36%) and only a few where LUM has higher estimates compared to IMAGE (notably the Netherlands with 15%).

The managed forest categories are fairly well aligned (R^2=0.94), although there are a number of outliers. Especially in Spain, the LUM database shows quite a bit higher forest management area compared to IMAGE. As Spain shows an opposite pattern for other natural land, where IMAGE has a higher estimate compared to LUM, this may originate from differences in the underlying land cover dataset regarding the classification of forest vs. non-forest in ESA-CCI and Corine. Other natural land has slightly lower agreement (R^2=0.90) partly due to the mismatch in Spain.

Built-up area has very low agreement between the LUM database and IMAGE (R^2=0.42), with LUM typically showing higher estimates compared to IMAGE. This again comes down to the underlying datasets of the global human settlement layer for IMAGE and Corine for LUM, where Corine identifies larger areas as built-up, possibly due to its higher spatial resolution.

The IMAGE 'other anthropogenic land' category is equated to the 'leftover cropland' and 'leftover grassland' categories in the LUM database. For LUM, these are the difference between the Eurostat cropland and grassland statistics and the respective land cover areas according to Corine. In the IMAGE dataset, a similar method is applied with the difference between the HYDE/FAO data and the agricultural land cover according to ESA-CCI. IMAGE overall shows higher estimates of this category compared to LUM (respectively 42 and 23 Mha in the EU), but the difference is not completely off the chart. However, at the NUTS2 level, the agreement is low (R^2=0.61).

Lastly, ice and natural forest are both small categories in Europe. Ice shows good agreement between the datasets. Natural forest is only present in a few NUTS2 regions in IMAGE, while it is present in a larger number of NUTS2 regions in the LUM database.

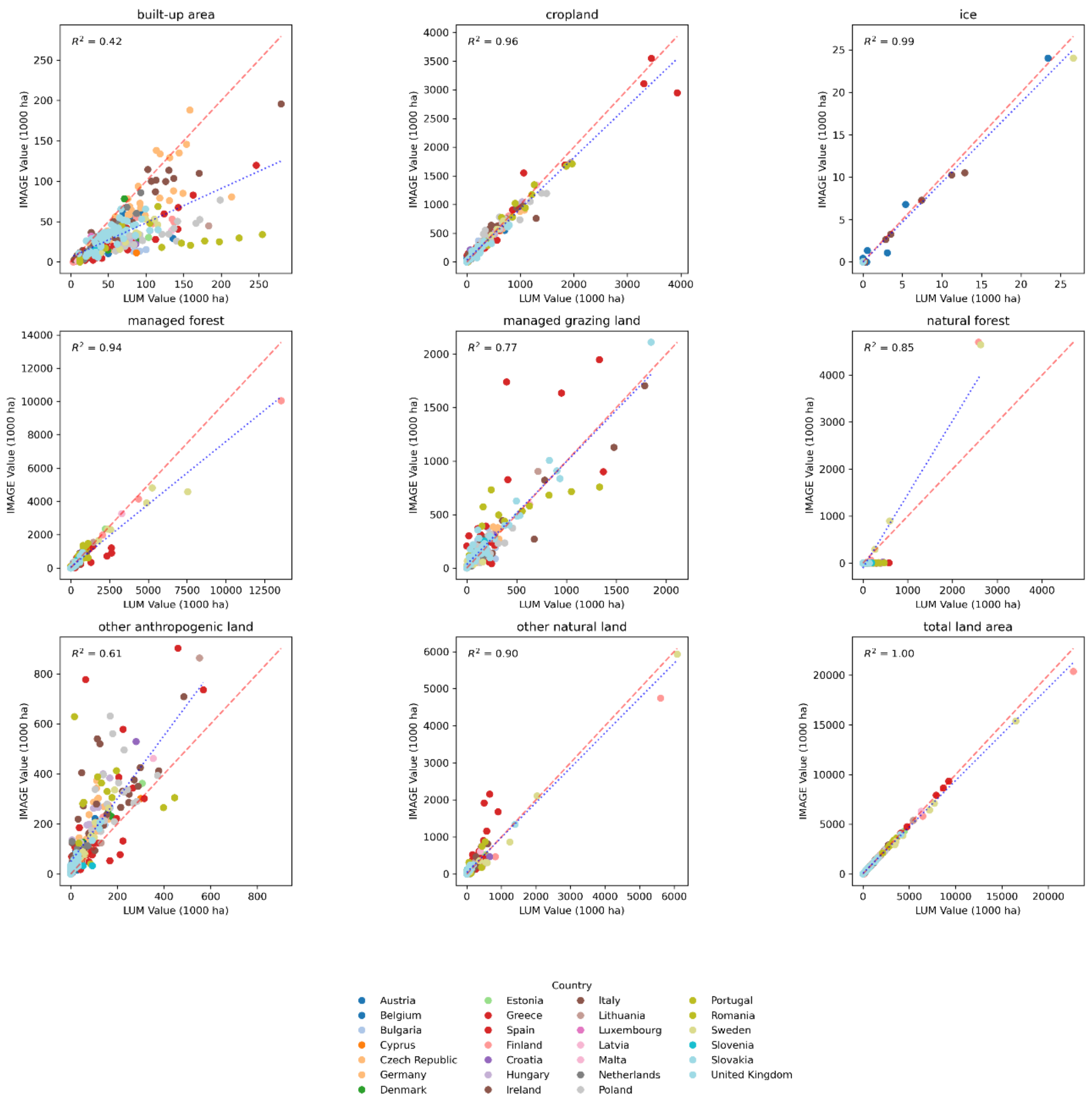

Figure 4: Scatter plots per land-use/cover category of LUM database and IMAGE/MAGNET dataset values by NUTS2 region.

Note: Each point is one NUTS2 region; colours depict the country in which each NUTS2 region is located. The pink dashed line is the 'perfect' 1:1 reference; the blue dotted line is the least-squares linear regression line, with the respective R^2-value in the top-left corner indicating the goodness of fit. R^2 is computed on levels and is therefore influenced by differences in region size; the 1:1 line is the more informative reference for systematic bias.

Overall, the comparison confirms that the two datasets are broadly consistent for the categories that dominate the European land balance — total area, cropland, managed forest, other natural land and ice — while the remaining differences are concentrated in built-up area, managed grazing land and other anthropogenic land. These are the categories whose definitions depend most strongly on the underlying land-cover product (Corine versus ESA-CCI) and on the reconciliation of land cover with agricultural statistics, rather than on genuine disagreement about land use. Replacing the IMAGE/MAGNET land-use/cover data with the LUM geodatabase for Europe is therefore feasible in principle, but it would introduce an inconsistency between the European and the global parts of a single global dataset. For this reason, the LUM geodatabase is used here to validate the existing IMAGE/MAGNET representation rather than to replace it; a full replacement would require harmonising the definitions of built-up and other anthropogenic land across the two products.

3. Encoding European policy instruments and incentives in macro-level models

This chapter documents how European agricultural and environmental policy instruments are represented in the three macro-level models. CAPRI provides the most detailed representation: its premium module encodes the CAP Strategic Plans intervention by intervention at NUTS2 level, and links agri-environmental payments to endogenous farm practices. GLOBIOM takes over the resulting payment rates and budget ceilings from CAPRI and applies them to its own crop and livestock activities, so that the two models share a consistent policy baseline. MAGNET represents the CAP more aggregately, through Pillar 1 and Pillar 2 subsidy categories whose effects on factor productivity are parameterised from the econometric literature.

3.1. THE CAPRI PREMIUM MODULE

The premium module of CAPRI (Common Agricultural Policy Regionalized Impact) simulates the full breadth of direct payments under the EU Common Agricultural Policy (CAP) (Britz and Witzke, 2014). It covers both Pillar I instruments — coupled and decoupled subsidies — as well as the main Pillar II measures. The module has evolved incrementally alongside successive CAP reforms: the Mid-Term Review (MTR, 2003), the Health Check (2008), the CAP 2014–2020, and lately the CAP Strategic Plans (CSPs) 2023-2028. Each reform layer has been incorporated while preserving the ability to simulate historical policy regimes. This cumulative structure enables CAPRI to represent both legacy instruments and newer policy elements such as payment convergence, greening requirements, and Good Agricultural and Environmental Conditions (GAECs).

A key CAPRI design principle is that premium definitions in the model closely follow the structure of the legal texts. This facilitates a transparent correspondence between model parameters and regulatory provisions. In addition, CAPRI's high level of spatial disaggregation — representing production activities at the NUTS2 regional level - facilitates the implementation of complex, geographically differentiated payment rules.

3.1.1. Basic concept of a premium scheme

In CAPRI, premiums are always linked to activity levels: per hectare in the case of crops and per head for livestock. Payments are computed from premium schemes, each representing a logical policy entity comprising:

- an application type (e.g., per hectare/head, per slaughtered head, per unit of output, or per livestock unit);
- a geographic scope (region or regional aggregate);
- nominal payment rates (PRMR) for one or more activity groups;
- ceilings on eligible entitlements (CEILLEV) and on total budget (CEILVAL).

The nominal payment rate (PRMR) is converted into a declared rate per hectare or head (PRMD) according to the application type. Payments are then spatially disaggregated from the EU or Member State level down to NUTS2 regions. When ceilings are binding, CAPRI applies an iterative premium-cut routine that proportionally reduces payment rates across all eligible activities. The resulting effective premium (PRME) is subsequently used in the supply model objective function.

3.1.2. The ceiling and premium-cut mechanism

The enforcement of ceilings constitutes one of the most complex components of the premium module. Because production quantities — and hence the total amount claimed under a premium scheme — are endogenously determined within the supply model, ceilings cannot be imposed directly during optimization. Instead, they are evaluated and enforced iteratively between model iterations.

Within a single model run, activity levels (hectares, heads) are treated as decision variables, while premium payments enter the objective function as exogenous revenues per unit of activity. Because these premiums remain fixed during optimisation, the model does not to internalise the fact that marginal premium revenues effectively drop to zero once a ceiling is reached. Without correction, this would lead to an overestimation of activities that are close to their ceiling.

To address this issue, CAPRI uses an iterative adjustment procedure. During each supply model run, the effective premium (PRME) is treated as a fixed, exogenous parameter. After the optimisation, total claims (PRME multiplied by activity levels) are compared with the relevant ceilings. Where ceilings are exceeded, premium rates are proportionally reduced, and the model is solved again. The loop continues until simulated claims under each premium scheme are consistent with the applicable entitlement and budget ceilings.

3.2. CAP POLICY UPDATE IN CAPRI

The 2023 CAP reform fundamentally restructured the way EU agricultural support is designed and reported. Instead of EU-wide regulations specifying uniform payment rates, Member States now submit individual CAP Strategic Plans (CSPs), which define the interventions, their target beneficiaries, and the PUAs — the payment rates per eligible unit — for each measure. This shift to a plan-based architecture required a comprehensive update of the CAPRI premium module.

The primary data input for the current CAP period is the CSPs Master File (Isbasoiu and Fellmann, 2024), a consolidated database that collects the intervention definitions and PUAs submitted by all Member States. CAPRI's premium module was adapted, modified, and updated to ingest this file as its policy input, replacing the previous approach of encoding payment parameters directly from EU regulatory texts (Fellmann et al., 2025). The module now integrates interventions and planned unit amounts for:

- All Pillar I direct payments, including both decoupled area payments (Basic Income Support for Sustainability — BISS) and Coupled Income Support (CIS) schemes.

- Selected Pillar II rural development interventions that can be represented within the model's supply-side framework, specifically Environmental, Climate-related and Other Management Commitments (ENVCLIM) and Natural or Other Area-Specific Constraints (ANC/LFA-type payments).

The CSP implementation in CAPRI preserves the model's core design principle: payment parameters are encoded to mirror the legal and programmatic definitions as closely as possible, ensuring that simulated payments are traceable to the underlying regulatory documents.

3.2.1. Mapping CSP interventions to CAPRI activities and regions

Translating CSP interventions into CAPRI premium parameters required a multi-dimensional matching exercise. The model's high spatial and sectoral disaggregation — with production activities resolved by NUTS2 region - means that each PUA from the CSP Master File must be linked to one or more specific CAPRI activities, at the appropriate spatial level.

The scale of this mapping task is substantial: approximately 1,000 PUAs from the direct payments and around 5,000 PUAs for ENVCLIM interventions were matched to the corresponding CAPRI production activities (Fellmann et al., 2025). The mapping involves several dimensions:

1. Intervention type to intervention and PUA: each intervention type (e.g., Eco-scheme, ENVCLIM, ANC) is linked to its specific interventions and the individual PUAs within each intervention. For example, the intervention type ECOS (Eco-scheme) in Austria is mapped to the intervention ECOS_AT_INV_31_01. And this intervention is mapped to the PUA "ECOS_AT_31_01_EB1" = Greening of arable land – cultivation of catch crops.
2. Territorial scope: PUAs are matched to the geographic level at which they are paid — national or regional (NUTS1/NUTS2). This is particularly important for Member States that have regionalised their CSPs, defining distinct payment rates in different parts of their territory.
3. Activity eligibility: decoupled area payments (BISS and related top-ups) are allocated to all eligible agricultural land and then attributed proportionally across agricultural activities. Coupled Income Support is modelled by assigning the PUA directly to the specific activities eligible for that support scheme (e.g., protein crops, suckler cows, specific fruit and vegetable sectors).
4. Budget and output matching: each PUA is associated with its planned budget envelope, the physical output unit (e.g., hectares, heads), and, where available, the planned output quantity at both PUA level and intervention level.
5. EU and national contributions: for Pillar II interventions, CAPRI's reporting framework was extended to separately record EU co-financing and national top-up contributions for each scheme. This preserves the distinction between EU budget expenditure and Member State co-financing in scenario output.

ANC payments (the successor to LFA payments) required additional mapping: each PUA was linked to the specific type of constrained area to which it applies, distinguishing between mountain areas, areas with significant natural constraints, and areas with specific constraints. This three-way categorisation reflects the regulatory structure of the current CAP and allows CAPRI to model differentiated payment rates by constraint type within a NUTS2 region. Figure 5 summarises how the CSP interventions are mapped onto CAPRI premium parameters.

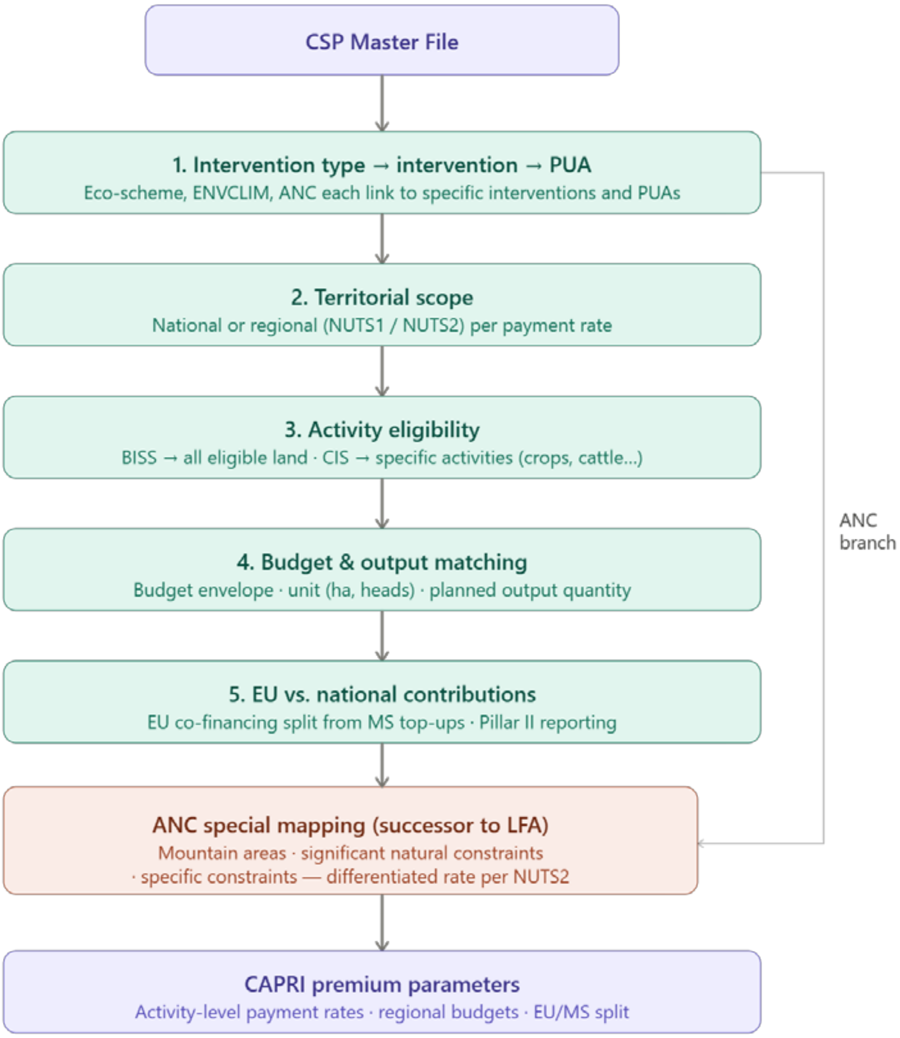

Figure 5: Mapping of CSP interventions to CAPRI premium parameters

Note: Own illustration. PUA = planned unit amount; ANC = Areas with Natural Constraints; LFA = Less Favoured Area.

3.2.2. Linking payments to endogenous mitigation technologies and farming practices

A distinctive feature of the CAPRI premium module is its ability to connect agri-environmental payment schemes to endogenous mitigation technologies/farming practices within the supply model. This linkage allows the model to simulate the effect of environmental payments not merely as income transfers but as instruments that shift the relative attractiveness of production technologies with different environmental footprints.

The mechanism works by associating specific payment schemes — particularly Eco-schemes under Pillar I and ENVCLIM interventions under Pillar II — with farm practices that correspond to mitigation technologies in the CAPRI supply model. When a payment scheme is active, the effective premium rate for an activity is modified depending on whether the associated mitigation technology is adopted. The introduction of the current CAP required a substantial update of the farm practices classification underpinning this linkage (Schievano et al., 2023; Angileri et al., 2024).

A systematic labelling exercise was carried out to identify which Eco-scheme and ENVCLIM interventions — and, more specifically, which PUAs within those interventions — require or incentivise particular farm practices from the new taxonomy. The labelling distinguishes between:

- Obligatory commitments: practices that must be adopted as a condition for receiving the payment.
- Optional commitments: practices that are encouraged or incentivised but not strictly required for basic eligibility.

The labelling was conducted by JRC staff (units D4 and D5), supported by an external network of national partners from seven Member States: Hungary, Czech Republic, Slovakia, Denmark, Poland, Croatia, and Latvia (Fellmann et al., 2025).

The updated farm practices classification is linked to the set of mitigation technologies explicitly represented in the CAPRI supply model. The following technologies are currently included (Table 1):

Table 1: Mitigation technologies and farming practices represented in the CAPRI supply model

MITIGATION TECHNOLOGY/FARMING PRACTICE	DESCRIPTION
NtotLimit	Total N input limit per ha
NminLimit	Mineral N input limit
NmanLimit	Organic / manure N limit
LUperHaLimit	Max livestock units per ha
ferttime	Fertilizer timing restriction
AmmAppHE	High-efficiency ammonia application
AmmAppLE	Low-efficiency ammonia application
vrt_sruc	Variable rate / precision farming
precFarm	Precision farming – soil mapping
nitr_inh	Nitrification inhibitors
winterCov · consTill · noTill	Cover crops, conservation tillage, no tillage
Buffer strips ×4	Buffer strips along water courses
fallow	Fallow / peatland restoration

The linkage between payment schemes and mitigation technologies enables two modes of simulation: scenarios in which technologies/farm practices are activated alongside the associated payments (reflecting the expectation that farmers adopt the required practices to claim the premium), and counterfactual scenarios in which technologies are switched off such that the payments from the eco-schemes and ENVCLIM are paid as lumpsum per ha/head.

The current CAP introduced a reinforced conditionality framework as a prerequisite for receiving all direct payments. Farmers must comply with a set of GAEC standards, which define minimum land management requirements. CAPRI implements four of these standards to the extent that they can be represented within the model's supply-side structure. Table 2 summarises the four standards and their implementation.

Table 2: GAEC standards implemented in CAPRI

GAEC	STANDARD NAME	IMPLEMENTATION IN CAPRI
GAEC 1	Maintenance of permanent grassland based on its ratio to total agricultural area	Implemented as a supply model constraint limiting the decline of the permanent grassland share relative to a base-year ratio. Directly related to the greening grassland obligation of the previous CAP, extended under conditionality.
GAEC 4	Establishment of buffer strips along water courses	Represented via the buffer strips mitigation technology. When GAEC 4 is active, a minimum share of land adjacent to water courses must be allocated to buffer strip activities. Also linked to Eco-scheme and ENVCLIM labelling via the farm practices mapping.
GAEC 7	Crop rotation in arable land (except crops grown under water)	Modelled using the Shannon Diversity Index applied to annual crop activities within each supply model region. The index captures the degree of crop diversity, with a minimum threshold enforcing rotation requirements. Applicable to annual crops only; perennial crops and rice are excluded.
GAEC 8	Minimum share of arable land devoted to non-productive areas and features; retention of landscape features; ban on cutting hedges and trees during bird breeding season	Implemented through the non-productive area activities in the supply model (including ecological set-aside, field margins, and flowering strips). GAEC 4 is additionally and automatically addressed through the integration of mitigation technologies and their association with specific farming practices via the labelling exercise.

3.3. CAP POLICY UPDATE IN GLOBIOM

Policy payments differ across regions and agricultural activities. Rather than encoding them separately, GLOBIOM takes them from the premium module of the CAPRI model (Britz and Witzke, 2014). The advantage is that the payments already follow the definitions used in the legislation, and are available at the level of individual crop and livestock activities.

Each payment scheme can apply to several activities, with different rates, and each activity can receive support from several schemes.

Premiums are paid per unit of activity — per hectare of a crop or per animal — at NUTS2 level or at a more aggregated level. Each scheme carries two ceilings: one on the number of eligible hectares or animals (CEILLEV) and one on the total budget of the scheme (CEILVAL).

The ceilings are enforced after the supply model has been solved. The premium module first declares a payment rate per activity (PRMD), which the regional supply models take as given. Once these are solved, the module adds up the hectares and animals to which each scheme applies.

Multiplying those quantities by the declared rate gives the payment that would be due if there were no ceiling. Where that amount exceeds the ceiling, the rate is scaled down by a cut factor. The resulting effective premium (PRME) is the payment rate passed on to GLOBIOM.

GLOBIOM simulations are conducted in 10-year time steps starting in 2000. Accordingly, policy payment data for each policy period are generated during the baseline calibration process in CAPRI. The Mid-Term Review (MTR) CAP Policy payments are used for the period 2000-2010, the CAP 2014 greening reform payments for 2011-2020, and the CAP Strategic Plans payments for the period from 2021 to 2030 and beyond, assuming no further policy changes.

To derive these payment datasets, three different versions of the CAPRI model were run during the baseline calibration process, each reflecting a distinct policy framework and producing policy payments mapped to specific activity levels:

1. ECAMPA3 version, with baseyear 2008, calibrated until 2020 using the pol_input/mtr_rd.gms file as reference scenario.
2. Trunk version, with baseyear 2017, calibrated until 2030 using the pol_input/cap_after_2014/ref.gms as reference scenario.
3. CSP version, with baseyear 2017, calibrated until 2030 using the pol_input/cap_after_2023/ref.gms as reference scenario.

During the baseline run, CAPRI writes the payment data to an intermediate file (policy.gdx). It contains the effective premiums for all Pillar 1 and Pillar 2 payments by crop and livestock activity at NUTS2 and regional level, together with the corresponding ceiling values for each policy measure by region.

The resulting, consistent payment data by region and activity is then mapped to GLOBIOM regions and activities. In addition, livestock payments are adjusted using the livestock unit (TLU) coefficients applied in GLOBIOM, as payments in CAPRI are defined per livestock unit. Finally, all payments are converted to USD at 2000 level, since CAPRI payments are originally calculated in euros and nominal value.

As shown in Table 3, payments (in 1000 USD per activity) are reported either as total direct payments (dptotal) or disaggregated by Pillar 1 and Pillar 2 payment schemes, as well as by specific direct or agro-ecological measures. Table 4 reports the corresponding budget ceilings (million USD) for each policy measure, at the aggregated level, by pillar, and by individual policy.

Table 3: Structure of policy payments in GLOBIOM, illustrative extract for Austria, Corn in 2000

PAYMENT SCHEME (PSDPAY)	PRME
DPFRMS	0.262439
DPRD_AE1	0.155618
DPRD_LFA	0.0833017
DPRD_N2K	0.000375565
DPPIL1	0.262439
DPPIL2	0.239295
DPAE	0.155618
DPSFP	0.262439
DPTOTAL	0.501734
dp_bps	0.186997
DPGREEN	0.0864624
DPYOUNG	0.00576416
DPRD_AE1	0.146959
DPRD_LFA	0.0803954
DPRD_N2K	0.000361443
DPPIL1	0.279223
DPPIL2	0.227716
DPAE	0.146959
natCeilCap14	0.279223
DPTOTAL	0.50694

Note: Extract of the p_premPaym parameter for Austria, corn, 2000 and 2020. PRME is the effective premium per hectare, expressed in 1000 USD per activity. The same structure applies to all regions, activities and policy periods. DPTOTAL is the total direct payment; DPPIL1 and DPPIL2 are the Pillar 1 and Pillar 2 aggregates.

Table 4: Budget ceilings by region and policy measure in GLOBIOM, illustrative extract for Austria, in 2000

PAYMENT SCHEME (PSDPAY)	CEILVAL
DPSCOW	71.5137
DPFRMS	710.486
dp68milk	13.2222
DPRD_AE1	177.339
DPRD_AE3	45.19
DPRD_AE4	13.7858
DPRD_AE5	204.859
DPRD_AE6	84.0622
DPRD_AE7	15.155

PAYMENT SCHEME (PSDPAY)	CEILVAL
DPRD_AE8	66.8705
DPRD_LFA	299.718
DPRD_N2K	1.26127
DPPIL1	795.222
DPPIL2	908.24
DP68	13.2222
DPAE	607.261
DPMTR	71.5137
DPSFP	710.486
DPTOTAL	1703.46

Note: Extract of the p_premData parameter for Austria, 2000. CEILVAL is the ceiling on total budget per premium scheme, in million USD. Ceilings for the CAP 2014 and CAP Strategic Plans periods follow the same structure, with the scheme codes of the respective policy period.

The CAP payments are introduced during model calibration rather than during the scenario runs, with the payments of the MTR period assigned to the calibration year 2000. They enter the model's welfare function as exogenous per-unit transfers, differentiated by payment scheme, and are attached to the crop and livestock activity variables across the full spatial and biophysical detail of the model: country, land class, agro-ecological zone, crop, and technology or animal type and production system. Payments enter in proportion to the activity level, which keeps them consistent with the CAP data definitions and leaves the existing land-use and livestock accounting of the model unchanged.

The implementation is controlled by a switch (EU_BASE) in 4_model.gms, which allows the user to activate (value 1) or deactivate (value 0) the CAP payments in a given model run.

Two sets of constraints accompany the payments. The first is a budget constraint per country and payment scheme: total CAP spending on crop and livestock activities may not exceed the budget defined for that intervention, which is taken from the CAPRI baseline described above. The second limits the activities eligible for payment to the physical bounds already present in the model, so that CAP-eligible area cannot exceed the crop area, and CAP-eligible herds cannot exceed the livestock numbers, that the model itself allows. Together, the two ensure that payments are granted only to production levels that are feasible, and prevent policy-induced expansion beyond the GLOBIOM baseline (implemented as MAX_CAP_EQU, MAX_AREA_EQU and MAX_HERD_EQU in 4_model.gms).

During the simulation period, policy payments from the relevant CAPRI baselines are applied according to the corresponding policy period. Payment levels beyond 2030 are assumed to remain constant and equal to those specified in the current CAPRI baseline covering the CAP Strategic Plans (CSP) policy period.

From 2030 onwards the payments are aggregated, to reduce model size and running time. In the CSPs each payment is differentiated by intervention type, intervention code and name, output indicator, territorial scope, planned unit amount and region, which yields almost 9,000 distinct payment categories. Aggregating them speeds up the optimisation while preserving the regional and activity-specific differences in support.

3.4. CAP IMPLEMENTATION IN MAGNET

MAGNET includes a dedicated module to represent the CAP, aggregating all relevant subsidy measures into two main categories: Pillar 1 and Pillar 2. Both pillars, and their sum, are integrated into the Social Accounting Matrix underlying the model, ensuring consistency with CSP and CATS data.

Pillar 1 defines the behaviour of decoupled and coupled direct payments, which are treated as subsidies entering the price composition at different leverage points. Decoupled payments (e.g. BISS, CRISS, eco-schemes, CIS-YF) are modelled as factor payments, which assume a subsidy solely on land in cases of full decoupling, or across multiple factors to allow production effects. Coupled and sectoral payments (e.g. CIS and sectoral interventions) are directly linked to activity-specific output, input or endowment variables. Both coupled and decoupled direct payments are assumed to have no effect on productivity.

Pillar 2 payments are introduced through five functional categories: human capital investments, physical capital investments, agro-environmental subsidies of the ENVCLIM type, ANC support, and wider rural development measures. Each category is linked to specific production factors (land, labour and/or capital) according to its nature.

In contrast to Pillar 1, the Pillar 2 measures captured in the MAGNET CAP module affect factor productivity. MAGNET incorporates these productivity impacts by assigning elasticities to different CAP payment categories, based on Khafagy and Vigani (2022) and additional expert judgement. Investment-type measures (human and physical capital, as well as wider rural development) are assigned a positive factor productivity elasticity of 0.03 (Khafagy and Vigani, 2022). Agro-environmental/ENVCLIM payments are assumed to have a negative land productivity elasticity of −0.024 (Khafagy and Vigani, 2022), i.e. a 1% increase in these payments reduces land productivity by 0.024%. ANC payments are assumed to have no direct productivity effect due to a lack of empirical evidence.

The CAP module has been designed to be compatible with the downscaled land supply and demand developed in the LAMASUS project. As an illustration, Figure 6 shows the distribution of coupled and decoupled CAP support across NUTS2 regions in 2050. Decoupled support is spread across all Member States and follows the distribution of agricultural area, whereas coupled support is concentrated in southern France, Spain, Italy and parts of central Europe, reflecting the sectors that Member States have chosen to support through coupled income support.

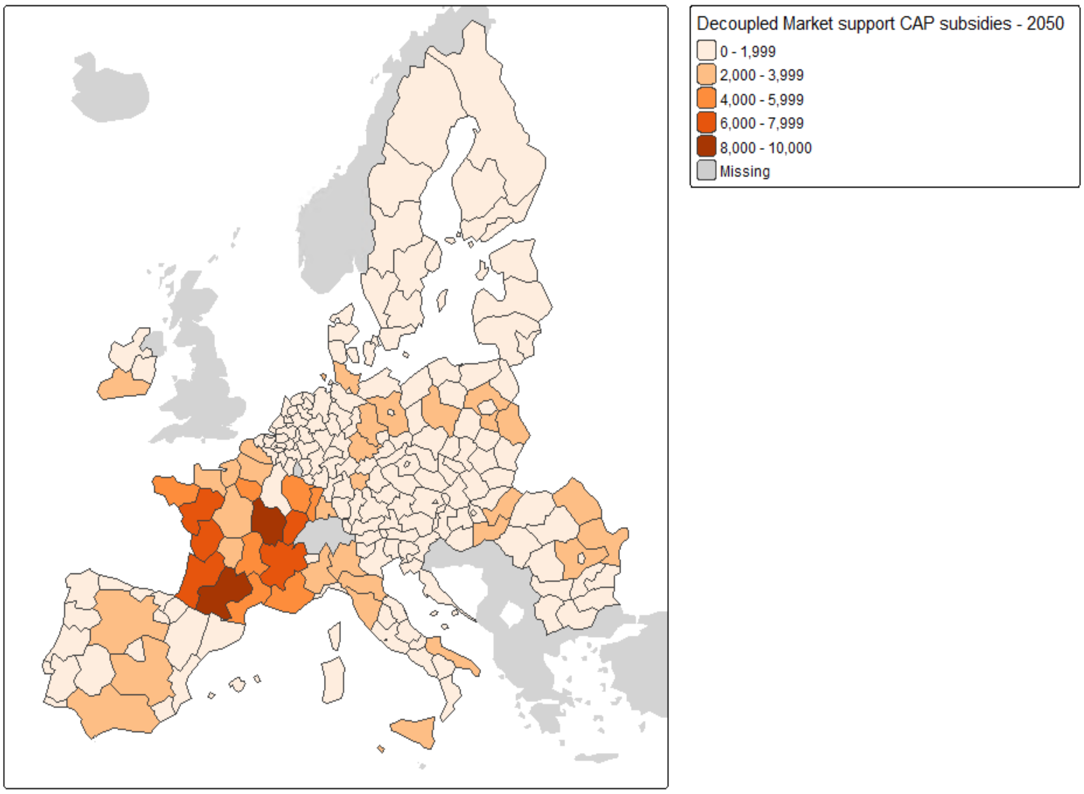

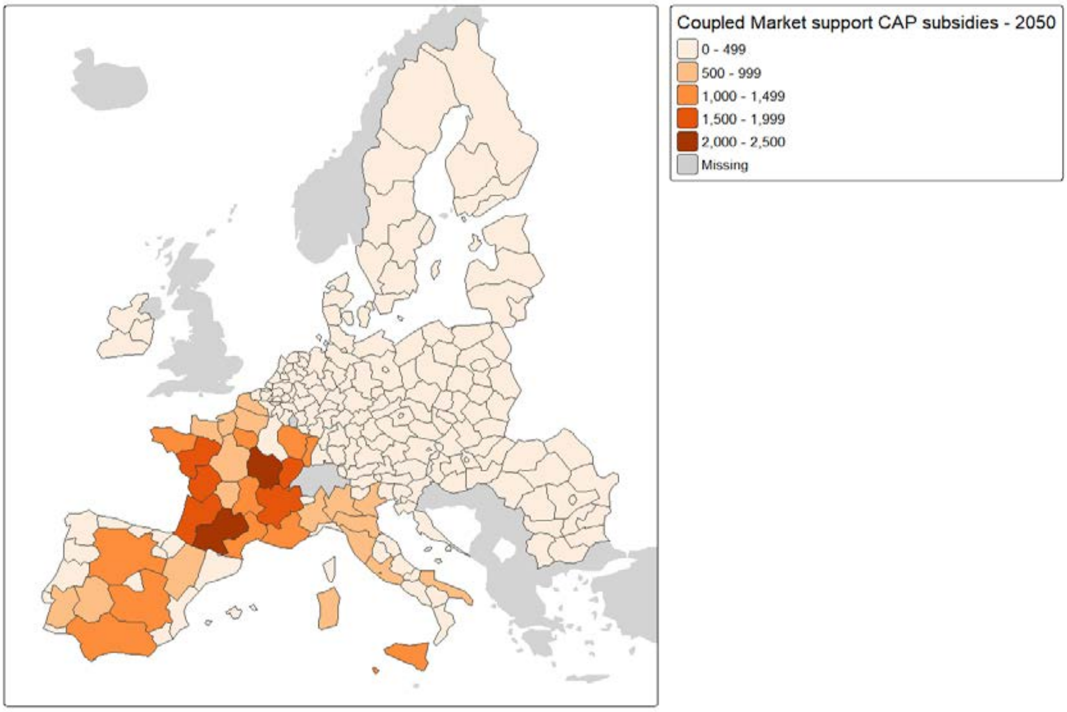

Figure 6: Coupled and decoupled CAP support by 2050 at NUTS2 level

4. Model capability extensions for land-use and land-use management systems

This chapter documents the land-use and land-use management systems that were newly represented, or refined, in the macro-level models. Four management domains are covered: organic farming and grassland management in CAPRI and GLOBIOM, climate-smart forest management in GLOBIOM/G4M together with an improved forestry representation in MAGNET, and peatland rewetting in all three modelling frameworks. For each domain the chapter describes how the management option is parameterised, which data sources underpin it, and how it enters the models' production, cost and emission accounting. Together these extensions allow the models to distinguish management regimes that were previously treated as homogeneous land-use classes.

4.1. ORGANIC FARMING

4.1.1. CAPRI implementation

CAPRI covers European countries with a set of about 250 programming models for each CAPRI NUTS2 region (which equals NUTS2 version 2006 for most countries). Organic agriculture is not yet endogenously represented, but the efforts to expand the model led to an ex-post database where agricultural activities are split by production system. Therefore, regional shares of organic agriculture are available by activity. The key raw data merged in the data consolidation includes Eurostat, IFS/FSS and FADN. The result of the data consolidation step are time-series of organic and conventional areas per crop and livestock activity as well as respective yields at NUTS2 level, allowing to explicitly calculate the organic crop shares in the historical database. As a side remark it may be stated for CAPRI that we relied on the supplementary information from Kremmydas et al. (2023) regarding the yield gaps between conventional and organic farming in the early development stage of implementing organic farming. The estimates are based on an FADN data and apart from the yield gap, they also provide estimates on differences between organic and conventional in terms of inputs and costs. Since we also use these estimates for consistency we decided at that time to also rely on the yield gaps until the CAPRI timeseries data becomes available. Apart from testing model performance and overcoming infeasibilities, a further advantage of the Kremmydas et al. (2023) yield gaps is that they also cover livestock activities and grassland. This allows livestock to be treated as organic activities as well, giving full coverage of the agricultural sector.

Organic shares for the historical period were determined from this database. For the forward-looking work, the land system change model CLUMondo, which draws on an organic farming certification database, was used to project the shares. The two sources were compared by regressing the organic shares at NUTS2 level, which showed a positive correlation (R2 of about 50%) in the regional dimension.

National target organic shares for the baseline, as agreed in the consortium, were regionalised using the CAPRI regional database and the CLUMondo regional pattern. Deviations from the baseline enter as regional shocks, defined as the difference between the regional target share and the regional baseline share.

These shocks were then translated into shocks for yields and input use as follows. For example, for a region where the yield gap for a crop is 40%, and the organic share for this crop increased from, 11% to 16%, this implies a 2% decline in the average yield (i.e., (16%-11%) x 40%).

The following assumptions for organic farms were made:

- Mineral fertilisers and pesticides use drops to zero suggesting that the decline in mineral fertiliser and pesticide use is on average in our example region 5%.
- For other inputs we used the cost differences to adjust other cost positions from Kremmydas et al. (2023).
- An increase in the organic share will trigger an increase in the baseline winter cover share.
- Organic yield gaps with respect to conventional using the regional CAPRI time series database.

4.1.2. GLOBIOM implementation

GLOBIOM is a global, recursive-dynamic partial equilibrium model of the agriculture and forestry sectors, which determines market equilibrium by maximising producer and consumer surplus. Its supply side is represented at the level of Simulation Units, clusters of grid cells sharing country, elevation, slope and soil characteristics (Skalský et al., 2008), with production technologies described through spatially explicit Leontief production functions. Macroeconomic drivers are taken from the SSP2 dataset with base year 2000 (Fricko et al., 2017; Hanasaki et al., 2013; O'Neill et al., 2020; Riahi et al., 2017), combined with agricultural projections from the Aglink-Cosimo model for 2010-2040 based on the 2023 Agricultural Outlook (Araujo Enciso et al., 2015; OECD/FAO, 2023).

In GLOBIOM, add-on technologies are represented as mitigation or productivity measures that are applied on top of existing production systems rather than replacing them. These technologies modify specific technical coefficients of an activity, such as emission factors, feed requirements, nutrient use, or yield parameters, while leaving the underlying production structure intact (IIASA, 2023). The model evaluates each measure based on its cost, technical potential, adoption ceiling, and compatibility with other measures. These characteristics define whether the technology is activated during the economic optimization of the system. GLOBIOM solves a welfare-maximizing optimization problem, where the objective function maximizes the sum of producer and consumer surplus minus production costs and technology-related costs. Add-on technologies enter this objective function as additional costed activities that modify the technical coefficients of the base production activity. When an add-on technology is available for activity a, GLOBIOM introduces a separate decision variable that represents applying that technology to a certain share or volume of activity a.

We represent organic farming in GLOBIOM as an add-on technology that modifies the performance of existing production systems. The add-on adjusts key technical coefficients, yield, production cost, and greenhouse-gas emissions, reflecting the empirical differences between organic and conventional systems. In addition, we define technical and economic applicability based on observed data from previous years for each commodity at the Member State level. Organic production typically shows lower yields but reduced reliance on synthetic fertilizers and pesticides. To capture these effects, we specify country-level parameters for yield gaps, emission factors, and cost differentials for all relevant EU crop and livestock systems.

The following section details the data sources used to construct these organic-farming parameters within the model extension. Additionally, we explicitly account for price premiums associated with organic production. Incorporating these premiums allows the modelling framework to capture not only the supply-side responses of organic farming systems, but also the demand-side effects driven by consumers' willingness-to-pay for organically produced goods. Specifically, we integrate crop- and livestock-specific organic price premiums into the model, reflecting empirical evidence that organic products command systematically higher market prices. This approach ensures a more comprehensive representation of market incentives shaping organic production decisions and improves the consistency of simulated outcomes with observed organic market behavior.

Several sources provide organic farming data on crop area, livestock numbers, production, trade and prices (Eurostat, 2024; FiBL, 2024; DGAGRI, 2024a, 2024b), but none covers all activities and regions consistently. We therefore use the organic farming time series of the CAPRI model up to 2018 at NUTS2 level, prepared during recent model development, as the primary source.

Organic yield gap data

We use for testing purposes the supplementary information from Kremmydas et al. (2023), whose estimates of the yield gap between organic and conventional farming are based on FADN data. The gaps are reported for five European regions: Central Europe North (Belgium, Luxembourg, the Netherlands, Germany, Poland), Central Europe South (Austria, Czechia, France, Hungary, Slovakia, Romania), Northern Europe (Sweden, Finland, Estonia, Lithuania, Latvia, Denmark), Southern Europe (Bulgaria, Croatia, Cyprus, Greece, Italy, Malta, Portugal, Spain, Slovenia) and the United Kingdom and Ireland.

Now when the CAPRI timeseries database is available the yield gaps between organic and conventional farms will be recalculated at NUTS2 level and more detailed crop and livestock production activities.

Organic costs

We use of an output of the IFM-CAP model in terms of cost estimates provided in Kremmydas et al., (2023). Modelling organic farming as mitigation technology doesn't allow us to distinguish between different input costs as it is reported in Table B1 in the paper. Instead, we calculated and aggregated input costs gaps between conventional and organic using the weights of the mean input cost in the table. For example, fully organic farm has fertilizers costs 221 euro/ha, other costs 414 euro/ha, plant protection area 228 euro/ha and seed costs 382 euro/ha, leading to shares: 0.18, 0.33, 0.18 and 0.31, respectively. These shares were used to multiply the estimated differences (gaps) per region of variable crop production costs between organic and conventional farms provided in Table A7. Regarding the crop and livestock production activity we also made use of the output of the IFM-CAP model per farm specialization from Table A7. Such as specialized horticulture farm estimates were multiplied with the shares of each cost category and the total was mapped to vegetable activities, specialized milk farms mapped to dairy cows, specialized granivores mapped to pig and poultry activities, etc.

Similar to yields, the cost structures for crop and livestock activities across regions will be updated using the final CAPRI time series for organic farming at the NUTS-2 level. But the information regarding the costs is still not completed as the area and yields.

Organic land-use shares

For organic land use shares we supplement the CAPRI timeseries data (2010 – 2018) with information from a recent publication by Pignotti et al. (2026) for 2010 and 2020.

As shown in Figure 7, the Pignotti database provides information by NUTS-2 region, year, and agricultural activity, including the area measured in hectares or livestock heads, disaggregated by specific farm types as well as the total. Using this database we calculated the share of organic farming by activity and region, which is used as the uptake of a mitigation technology in a specific period in the model.

		2010	2020
DK000000	SWHE	757660	502070
	SWHEorg	11427,3018549747	14180
	SWHEcon	746232,698145025	487890
	RYEM	51340	115160
	RYEMorg	7049,14839797639	20300
	RYEMcon	44290,8516020236	94860
	BARL	568070	652850
	BARLorg	13361,281618887	30310
	BARLcon	554708,718381113	622540
	OATS	41900	74770
	OATSorg	7367,15851602024	27800
	OATScon	34532,8414839798	46970
	MAIZ	9120	6210
	MAIZcon	9120	6210

Figure 7: Example of organic and conventional farming area (ha) per selected crops in Denmark in 2010 and 2020 from Pignotti et al. (2026)

Organic emissions accounting

GHG emissions for organic farming are derived from two main adjustments: the elimination of synthetic fertiliser use and the increase in emissions associated with greater reliance on manure-based nutrients. The removal of synthetic fertilisers reduces upstream and field-level emissions linked to nitrogen manufacture and application, while the higher share of manure contributes additional nitrous oxide and methane emissions, depending on management practices and nutrient availability. The resulting emission factor for organic production, therefore, reflects the net outcome of reduced synthetic inputs and increased manure-related emissions.

4.2. GRASSLAND MANAGEMENT

4.2.1. Importance of grassland management for climate policy

In Europe, grasslands play a crucial role in providing a range of ecosystem services, including biodiversity conservation, soil erosion prevention, carbon sequestration, and the preservation of the aesthetic and cultural value of rural landscapes (van den Pol-van Dasselaar et al., 2019). Sustainable management of grasslands has acquired increasing significance in the European Union (EU) to achieve the objectives of the Common Agriculture Policy (CAP). The CAP policy of the European Union sets standards on good agricultural and environmental conditions of land (GAEC). These conditionalities are set by the EU for farmers as basic rules to respect, in order to receive EU income support. These conditionalities target grasslands through two GAECs: *maintain a certain share of permanent grassland of the total agricultural area* (GAEC 1), and *protect environmentally sensitive permanent grasslands in Natura 2000 sites* (GAEC 9) (European Commission, 2025). It is therefore important to have sustainable management of grasslands, which includes improvement in grassland management and the intensity of grassland use.

4.2.2. GLOBIOM coverage of grassland

In GLOBIOM, previously, grassland areas were not distinguished according to management intensity, and therefore the total area was considered. As part of the LAMASUS project, we introduced a classification system that separates grasslands into High Input (HI) and Low Input (LI) systems for grasslands. The grassland classification is based on the LUM Geodatabase[1] and yield and fertiliser use data were developed from the EPIC Model, which also utilises the Geodatabase as a core input parameter to understand production and emissions.

To create the HI and LI grassland classification, we developed a mapping between the LUM classes and the GLOBIOM grassland classes. Table 5 shows the link between the LUM classes and the associated GLOBIOM grassland management class.

Table 5: Mapping the LUM land classes to GLOBIOM land classes

CODE	LABEL	GLOBIOM LAND CLASSES
15	Very high-density managed pasture	
16	High-density managed pasture system	
19	Very high-density managed grassland	High-Input Grassland
20	High-density managed grassland	
4012	Intensive heterogeneous grassland classes	
14	Agroforestry	
17	Moderate-density managed pasture system	
18	Low-density managed pasture system	
21	Moderate-density managed grassland	
22	Low-density managed grassland	
23	Rough grazing	Low-Input Grassland
24	Silvo-pastoral agroforestry	
25	Managed semi-natural and natural grassland	
26	Unmanaged semi-natural and natural grassland	
4013	Extensive heterogeneous grassland classes	

Using the databases above, GLOBIOM calculates the following:

1. Area and yields based on Simulation Units, which are then aggregated to the Country, LUID, Soil, slope, altitude and AEZ classifications at the HI and LI systems
2. Fertilizer use at the Simulation Units, which is then aggregated to the Country, LUID, Soil, slope, altitude and AEZ classifications at the HI and LI systems
3. Grassland technologies, which include silvopasture aggregated at the country level for HI and LI systems.

Click or tap here to enter text.Grasslands in the European Union are classified by management intensity — mowing frequency, fertilisation and grazing pressure (Bai and Cotrufo, 2022; Estel et al., 2018) — and by livestock numbers and the extent of extensive grazing. Climate and soil conditions add further variation across the Union (Schils et al., 2022).

Extensification, that is a reduction in management intensity, is widely regarded as a route to more sustainable grassland use, since many European grasslands are overused and overfertilised, which reduces biodiversity and their capacity to act as carbon sinks (Humann-Guilleminot et al., 2023; Schreiner et al., 2026). Silvopasture, the integration of trees into grassland, is a further option; it is the most widespread agroforestry practice in Europe, reaching up to 37% of the land in some regions (Rodriguez-Rigueiro et al., 2021). Both options are represented in GLOBIOM through the high- and low-input grassland systems described above.

4.2.3. CAPRI coverage of grassland

Grassland is a central production activity in the CAPRI model — it generates the bulk of roughage used by ruminant livestock, and its management intensity directly determines the nitrogen balance, greenhouse gas emissions, and biodiversity outcomes simulated in policy scenarios. Despite its importance, the historical treatment of grassland in CAPRI has rested on a coarse, data-constrained dichotomy: the total grassland area of each Member State is split equally between intensive grassland (GRAI) and extensive grassland (GRAE), with a fixed 50:50 ratio applied uniformly across all NUTS2 regions. This default has long been recognised as a simplification that limits the model's ability to represent the true spatial distribution of grassland management intensity across the EU.

Similar to GLOBIOM, using the LUM database for 2018, the fixed 50:50 grassland split has been updated. The LAMASUS 12-class system is mapped to five productive grassland classes (Table 6). These five classes span the range from very intensive to very extensive management and are designed to bridge between the LAMASUS spatial data and the two endogenous CAPRI activities GRAI and GRAE:

Table 6: Mapping between the LUMs, the grassland classes and CAPRI grass activities

CAPRI GAMS CODE	LUM GAMS CODE	FULL NAME	LAMASUS CLASSES INCLUDED	INTENSITY LEVEL
GRAI	PMEAI	Intensive permanent meadows	Classes 1-2 (very high and high management intensity in managed grazing areas)	Very high / high
GRAE	PMEAE	Extensive permanent meadows	Classes 3-4 (moderate and low density, in managed grazing areas)	Moderate / low
GRAI	PPASI	Intensive permanent pastures	Classes 5-6 (very high and high management intensity, outside managed grazing areas)	Very high / high
GRAE	PPASE	Extensive permanent pastures	Classes 7-8 (moderate and low density, outside managed grazing areas)	Moderate / low
GRAE	PPASV	Very extensive permanent pastures	Classes 9, 10, and 11 (rough grazing, silvo-pastoral, managed semi-natural)	Very low / rough grazing

The mappings from Table 6 allow us to calculate the respective shares which are then applied to the total Member State grassland area to obtain the area of each productive[i] grassland class. This produces, for each Member State and each productive class, the area (in 1,000 ha). Then the five LAMASUS-derived classes in 1000 ha are summed into the two endogenous CAPRI supply model activities (GRAI and GRAE) using the mapping from column one.

The five productive grassland classes are assigned differentiated yields, reflecting the empirical relationship between management intensity and forage production. Yields are derived from the Member State average GRAS yield by applying class-specific yield factors as priors: The resulting factors are given in Table 7.

Table 7: Prior yield factors assigned to the five productive grassland classes

CLASS	PRIOR YIELD FACTOR RELATIVE TO MS AVERAGE	INTERPRETATION
PMEAI	1.5	Intensive permanent meadows produce 50% more than the MS average (cutting 3–4 times per year, high nitrogen input)
PMEAE	0.8	Extensive permanent meadows produce 80% of the MS average (1–2 cuts per year, limited inputs)
PPASI	1.4	Intensive permanent pastures produce 40% more than the MS average (high stocking density, managed)

[i] Productive is defined as grassland classes which have yields in contrast to grassland without yields (G0YLD) in the LUM database.

CLASS	PRIOR YIELD FACTOR RELATIVE TO MS AVERAGE	INTERPRETATION
PPASE	0.7	Extensive permanent pastures produce 70% of the MS average (moderate stocking, limited management)
PPASV	0.2	Very extensive permanent pastures produce only 20% of the MS average (rough grazing, semi-natural, minimal management)

These prior yields are then used to calculate a weighted sum of the grass yields at Member State level. These new updated yields are used to define a scaling factor against the old grassland yields. The scaling factor is then multiplied by the specific GRAE and GRAI yields.

As described, by using the LUM database we produce a grassland intensity split at Member State level. The CAPRI supply model, however, operates at the NUTS2 level. Hence, in the current implementation, the MS-level area and yield ratios derived from the LAMASUS data are applied uniformly to all NUTS2 regions within a Member State. Applying the LAMASUS database resulted in a pronounced shift in the EU-wide grassland intensity composition, approximately 20:80 compared to the 50:50 split. Meaning only about 20% of total EU grassland is classified as intensive (GRAI), while 80% is extensive (GRAE). This reflects the empirical reality that the majority of EU grassland, when assessed against management intensity data, falls into the moderate, low, or rough-grazing categories rather than the high-intensity managed category.

This shift has far-reaching implications for the behaviour of CAPRI in policy simulations, particularly those involving agri-environmental policies that incentivise extensification or impose nutrient reduction targets. Figure 8 shows, that imposing a more environmental ambition target in terms of nutrient surplus (reduction target of 25% in 2040 compared to the baseline) has resulted into a softer extensification impact in EU due to a large share of GRAE already in the new split.

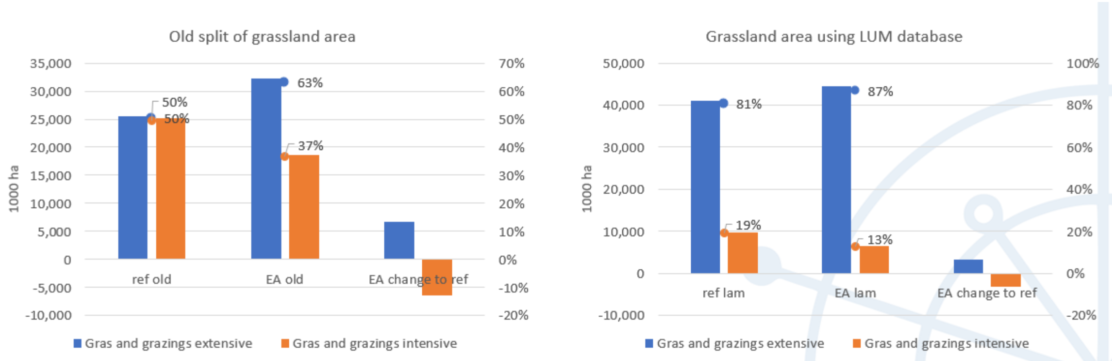

Figure 8: Disaggregation of extensive and intensive grassland before and after using LUM database in CAPRI and corresponding area changes in N surplus scenario

Although improved grassland disaggregation with the updated database improves the grassland representation, the most significant limitation of the current implementation is that the LAMASUS-derived area shares are applied uniformly (as priors) within each Member

State. Meaning all NUTS2 regions in each MS receive the same GRAI/GRAE ratio. This is because the CAPRI database calculation works at the MS level but also the absence of data at NUTS2 level that can be used during the regional database step. The LAMASUS database itself contains gridded spatial data that could in principle be aggregated to NUTS2 level, producing NUTS2-specific intensity shares. This would eliminate the within-MS homogeneity assumption and allow the model to represent the true sub-national variation in grassland management intensity — for example, the contrast between the highly intensive grassland of Flanders and the extensive grassland of the Ardennes, both within Belgium.

4.3. FOREST MANAGEMENT

4.3.1. Climate-smart forest management systems in GLOBIOM

The climate-smart concept originated in agriculture (FAO, 2010) and was extended to forestry by Nabuurs et al. (2017, 2018), who define climate-smart forestry (CSF) as a strategy aimed at increasing the climate benefits of forests. CSF covers management practices such as improving the climate resilience of forests, restoring forest ecosystems, reducing the risk of natural disturbances, and using wood-based products to substitute fossil fuels, and it considers the whole value chain from forests to material products and bioenergy. Because several of these effects are accounted for outside the forest sector under IPCC and UNFCCC rules, the overall climate impact of forests is difficult to capture in a single figure (Petersson et al., 2022; Verkerk et al., 2020).The climate-smart concept originated in agriculture (FAO, 2010) and was extended to forestry by Nabuurs et al. (2017, 2018), who define climate-smart forestry (CSF) as a strategy to increase the climate benefits of forests. CSF spans the whole value chain, from forest management to wood-based material products and bioenergy, including substitution effects. Several of these effects are accounted for outside the forest sector under IPCC and UNFCCC rules, which makes the overall climate impact of forests difficult to capture in a single figure (Petersson et al., 2022; Verkerk et al., 2020).

Applying climate-smart forest management to GLOBIOM

There is no single, universally adopted definition of CSF, and as a large-scale land-use model GLOBIOM has limited ability to represent detailed silvicultural practices (Bowditch et al., 2020). We therefore apply a simplified CSF approach in which the forest-sector carbon components are modelled separately.

In this framework, forest-sector carbon modelling is separated into four components: forest carbon, harvest wood products (HWP), bioenergy with carbon capture and storage (BECCS) and substitution effect (SUBST). Forest carbon refers to biogenic carbon stored in forest biomass. HWP and BECCS represent biogenic carbon stored outside forests, while SUBST capture changes in fossil carbon storage resulting from the use of wood-based products to replace fossil-based products.

Forest carbon is future separated into two components: forest management and forest area change. Forest management covers “forest land remaining forest land” and is modelled based on age-class dynamics and harvest volumes. Forest area change captures emissions from deforestation and carbon uptake from afforestation.

Under IPCC and UNFCCC carbon accounting rules, BECCS and SUBST are attributed to sectors other than forestry. The approach applied here can therefore be read as an extended biogenic carbon accounting framework that combines life-cycle assessment methods and energy-model outputs with the usual IPCC and UNFCCC guidelines.

Modelling forest-based biogenic carbon in forests and outside forests

Age-class dynamics

Forest age-class dynamics in GLOBIOM works similarly than in large-scale area-based matrix models such as the European Forestry Dynamics Model (EFDM) (Packalen et al., 2014) or the European Forest Information Scenario Model (EFISCEN) (Schelhaas et al., 2007). The main difference between GLOBIOM and these models is that harvest decisions and age-class dynamics are based on economic optimization instead of statistical transition probabilities.

In GLOBIOM the choice among management systems and age classes is made independently for each grid cell. A cell consists of several even-aged stands divided into discrete age cohorts; after each simulation period, stands move to the next cohort and their biomass grows accordingly, while harvested stands return to the youngest cohort. Harvest and management decisions are therefore taken jointly with the age-class structure.

For the historical period 2000-2020, forest carbon stocks are calibrated to FRA (2020) data and downscaled to the grid level using information from the G4M model (Kindermann et al., 2006, 2008) and a global age-class database (Besnard et al., 2021). After 2020, forest carbon stocks are determined endogenously through the model's age-class dynamics, which develop endogenously in response to harvest volumes, growth curves, natural mortality, and forest area changes (deforestation/afforestation).

To ensure the long-term sustainability of harvest volumes in the recursive dynamic framework, the model imposes two additional constraints. First, harvested biomass in each grid cell cannot exceed biomass growth. Second, harvesting is restricted to age classes older than the optimal rotation time. For EU forests, optimal rotation ages typically range between 60 and 100 years, depending on roundwood demand.

Because FRA (2020) data do not capture the observed decline in the EU forest carbon sink after 2015, more recent data from the EEA (2025) are used for EU countries to better reflect recent developments. Using this method, the EU forest carbon pool is estimated to be a sink of about 253 MtCO2/yr in 2020, closely matching the official EU LULUCF estimate of 257 MtCO2/yr (EEA, 2025).

Age-class dynamics imply that harvest levels have a direct, time-dependent effect on forest carbon stocks. The effect is largest in the short run and diminishes over time, as regrowth compensates for the carbon sequestration lost through harvesting; it is larger at high than at low harvest levels, because higher harvest intensity shortens rotations; and it is smaller where forest management is more efficient, that is, where a larger share of the living biomass is harvestable roundwood.

The magnitude of this effect can be summarised by the carbon balance indicator (CBI) used in the life-cycle assessment literature (Soimakallio et al., 2022), defined as the change in the forest carbon sink divided by the change in harvest volumes. In GLOBIOM, CBI is around 1.6 in 2030, consistent with published estimates for temperate and boreal forests, and converges towards zero as the age-class structure reaches a new steady state. The response is asymmetric: increases in harvest produce larger CBI values than comparable decreases.

Afforestation and deforestation

Forest area change is separated into afforestation and deforestation, both accounted for relative to the base year 2000. For 2000-2020 the areas are taken from FRA (2020) country-level data; from 2020 onwards they are taken from G4M country-level areas for the RCP4.5 mitigation scenario (Kindermann et al., 2006, 2008; IIASA, 2018). In both cases the country totals are allocated to the grid according to GLOBIOM forest land use and management dynamics. Afforestation is reported as a positive and deforestation as a negative cumulative area change relative to 2000 (Figure 9).

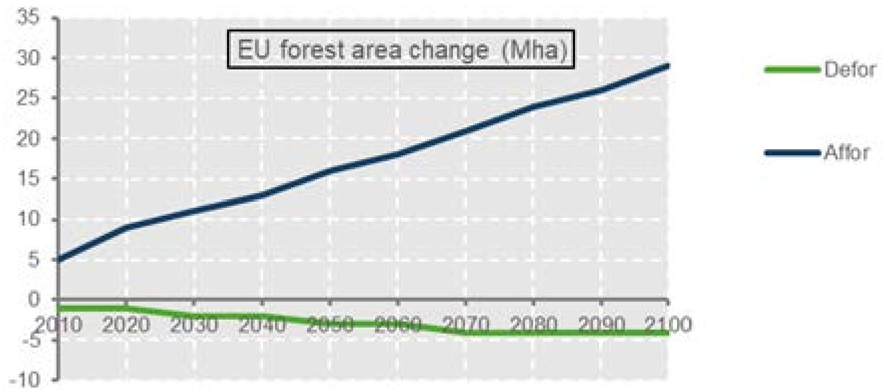

Figure 9: EU-level cumulative forest area change for afforestation and deforestation

Deforestation emissions are calculated from the loss of living biomass resulting from the conversion of forest land to agricultural land, while afforestation uptake is modelled using age-class dynamics similar to those applied for forest management emissions. For simplicity, afforested areas are assumed to be managed exclusively for carbon sequestration and are therefore not eligible for harvesting.

HWP and BECCS

Harvested wood products (HWP) carbon accounting follows the IPCC production approach (PA), which is the most commonly used methodology to calculate HWP carbon storage (IPCC, 2019). The initial HWP carbon pool is calculated using HWP production and trade data from the FAOSTAT database covering the period 1961 to 2020 (FAO, 2025). Based on this approach, the EU HWP pool acted as a sink of about 35 $MtCO_2$/yr in 2020, which is close to the official EU LULUCF estimate of 38 $MtCO_2$/yr (EEA, 2025).

HWP carbon storage and its sink are considerably smaller than those of forest carbon — typically about 5% of forest aboveground carbon storage and about 10% of the forest carbon sink (Johnston and Radeloff, 2019; Zhao et al., 2022) — because roughly 75% of tree biomass is lost as harvest and industry residues, and because product lifetimes are shorter than tree lifetimes.

Bioenergy with carbon capture and storage (BECCS) is accounted for alongside HWP. The difference between the two lies in permanence: HWP have half-lives of up to 35 years, whereas BECCS storage is assumed permanent. The share of bioenergy equipped with BECCS is taken from the MESSAGE model and rises from about 5% in 2030 to 75% in 2100, with an average carbon capture rate of 63% (IIASA, 2018).

In this deliverable, the amount of BECCS for the EU is calibrated to match PRIMES model estimates by adjusting both the BECCS carbon capture rates and the share of bioenergy equipped with BECCS.

Substitution effects

The substitution effect refers to the use of wood-based products to replace fossil-based products and therefore reduce fossil CO2 emissions. In this study, the substitution effect is modelled using production volumes of semi-finished wood products combined with displacement factors (DFs) from the literature (e.g., Leskinen et al., 2018; Myllyviita et al., 2021; Niemi et al., 2025).

The substitution effect is calculated as an additional effect, that is, relative to a reference that already includes the forest industry, rather than against a hypothetical no-forest-industry situation. It can therefore be positive or negative, depending on whether the consumption of wood-based products rises or falls relative to the reference.

The substitution effect is assumed to be dynamic over time, reflecting expected decarbonization pathways. Accordingly, DFs are assumed to decrease over time as fossil-based production becomes less carbon-intensive (Brunet-Navarro et al., 2021; Niemi et al., 2025). In particular, we assume that DFs decrease in line with the EU net-zero mitigation path (Table 8).

Table 8: Displacement factors used for EU countries

WOOD CATEGORY	2020	2030	2040	2050	2060	2070	2080	2090	2100
Sawnwood	0.8	0.6	0.4	0.2	0.2	0.2	0.2	0.2	0.2
Plywood	0.7	0.6	0.5	0.4	0.4	0.4	0.4	0.4	0.4
Fiberboard	0.5	0.433	0.366	0.3	0.3	0.3	0.3	0.3	0.3
OW_biomass	0.8	0.6	0.4	0.2	0.2	0.2	0.2	0.2	0.2
EW_biomass (forest industry)	0.6	0.433	0.266	0.1	0.1	0.1	0.1	0.1	0.1
EW_biomass (bioenergy plant)	0.42	0.3031	0.1862	0.07	0.07	0.07	0.07	0.07	0.07
FW_biomass	0.4	0.266	0.133	0	0	0	0	0	0

WOOD CATEGORY	2020	2030	2040	2050	2060	2070	2080	2090	2100
Woodpulp	0.24	0.18	0.12	0.05	0.05	0.05	0.05	0.05	0.05
Dissolving pulp	0.86	0.64	0.43	0.2	0.2	0.2	0.2	0.2	0.2

Note: The decline in Displacement Factors over time is based on the EU net-zero mitigation pathway. EW = Energy wood (modern bioenergy), FW = Fuel wood (traditional bioenergy), OW = other roundwood.

The substitution effect is reported both as an annual flow of avoided CO2 fossil-fuel emissions and, by aggregating those flows, as a cumulative effect that can be compared with forest and HWP carbon stocks. A positive value indicates avoided fossil fuel use, meaning that fossil carbon remains in the ground because consumption of wood-based products increases; a negative value indicates the opposite. For the EU, the annual effect is estimated at between about +50 and −40 MtCO2/yr, which is consistent with other EU-level estimates (Brunet-Navarro et al., 2021; Jonsson et al., 2021).

4.3.2. Improved economic representation of forestry in MAGNET

The MAGNET forestry representation was expanded to capture harvested wood products and the paper & pulp sector in more detail, and to improve coherence with GLOBIOM, allowing for more detailed estimates of forest-based production and for cross-model comparison. The MAGNET model was recently expanded with more detailed HWP quantities in the ForestNavigator project and a more detailed economic representation of the paper & pulp sector by splitting it from the parent sector of paper, pulp & publishing in the MAGNET database.

In MAGNET, the forestry sector, responsible for producing primary materials, is represented as a single economic sector that uses land endowments as a factor input, that is, as a primary production factor alongside labour and capital. This land can compete directly with agricultural land, placing forestry in dynamic competition with agriculture. Several scenario implementation mechanisms have been developed to capture these real-world dynamics and improve consistency with GLOBIOM.

The first step aligns wood demand with GLOBIOM. Higher demand for wood products is simulated through subsidies on the intermediate use of wood in construction and of pulp in textiles, which raises timber demand indirectly, while substitution reduces demand for materials such as cement and steel. The relevant elasticities of substitution are set to match the GLOBIOM demand path.

The second step aligns the land response. MAGNET baselines show managed forest area increasing in the EU, because demand for forest products is sustained, agricultural land declines and forestry sits on a single land supply. GLOBIOM instead keeps managed forest area broadly stable and meets higher harvests through changes in management systems. MAGNET can be brought closer to this behaviour by constraining the land use of the primary forestry sector through a land endowment tax, which shifts the response towards higher harvest intensity achieved through capital and labour.

The third step approximates forest management dynamics, which MAGNET does not represent in the detail available in GLOBIOM. A yield shifter allows targeted changes in harvest intensity: yield is defined as the ratio of economic output to land demand, and making this variable exogenous while solving endogenously for a land-use efficiency parameter constrains the growth in output volume for a given landTwo works for me, demand. The shifter can also be set to follow a given path of harvest intensity over time.

4.4. PEATLAND REWETTING

4.4.1. CAPRI

Scenario work on peatland rewetting or histosol protection policies requires information on cropland and grassland areas separately on organic soils, emission coefficients for full or partial rewetting, cost information for rewetting efforts, and scenario assumptions in terms of area targets for protection measures or carbon prices to steer endogenous uptake.

Area of agricultural peatland

The current CAPRI information has been revised under the EUCLIMIT-6 and ECAMPA-4 projects in 2022-23. The basic information relates to the shares of cropland or grassland on organic soils at the regional level. This had been estimated by JRC.D5 staff following a procedure described in a technical document committed to the CAPRI svn repository (revision 9810). It combines country submissions of land use on organic soils to the UNFCCC, a map of organic soils derived from the Harmonized World Soil Database (FAO/IIASA/ISRIC/ISS-CAS/JRC, 2012), and CAPRI NUTS2 level crop data for the base year 2012 disaggregated to so-called Farm Structure Units (FSUs) using a special extract of Eurostat Farm Structure Survey crop information at 10 km2 grid level. The FSUs are spatial units created by the intersection of this 10 km2 grid, the NUTS2 regional borders and the soil mapping unit borders of the HWSD.

The estimation procedure put emphasis on preserving the soil map information while treating the UNFCCC submissions only as proxy information without a strict scaling. Both IMAGE and GLOBIOM rely on the European Wetland Map (EWM) as a basic source (see below) such that it is of interest to compare the current CAPRI data with other sources (Figure 10).

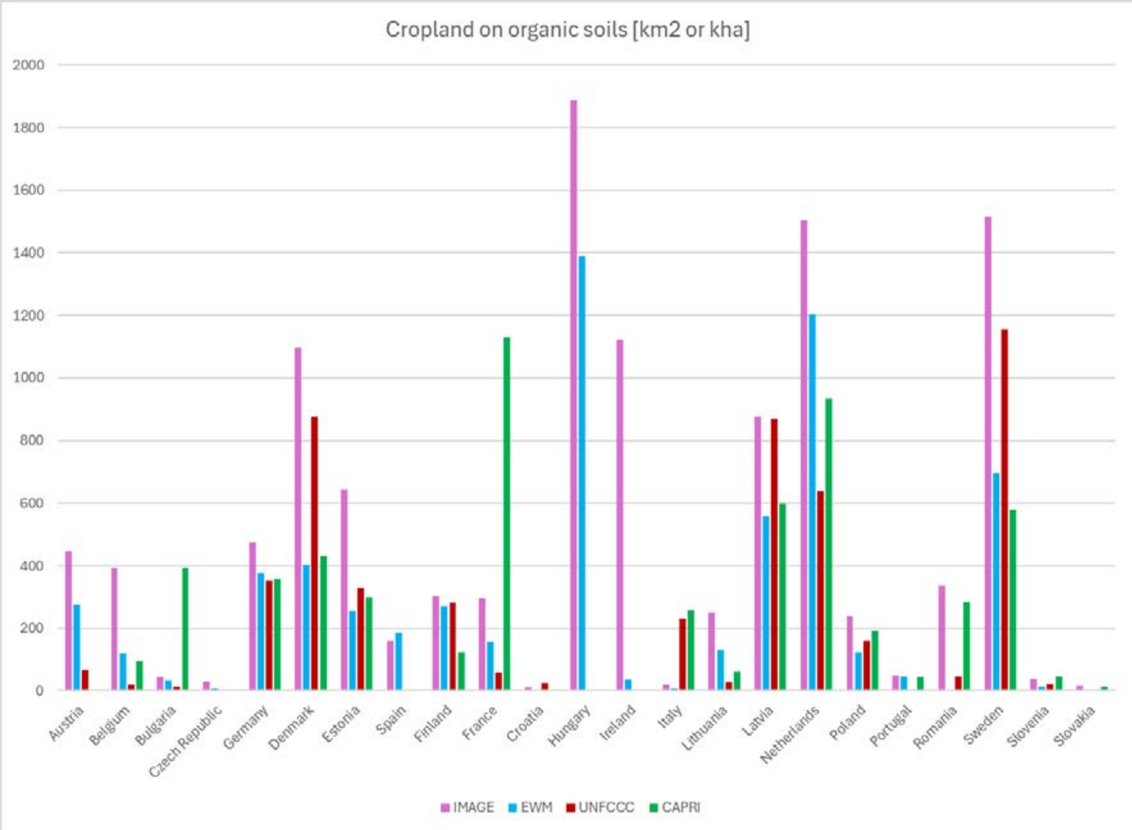

Figure 10: Cropland areas on organic soils according to different sources in km2, except for Germany, Finland, Lituania and Poland (all in kha)

Several observations may be made. CAPRI cropland on organic soils is well aligned with other sources for the important cases of Germany and Poland, but can also exceed them markedly, as for Bulgaria or France, while Finland and Austria are examples of strong downward deviations. The CAPRI data are only roughly aligned with the UNFCCC submissions, although in the cases of zero organic soil area (Spain, Hungary, Ireland) the two agree. Both the CAPRI and the UNFCCC areas are often lower than the IMAGE or EWM data.

Grassland on organic soils accounts for even larger areas than cropland. For grassland, CAPRI distinguishes productive grassland on organic soils from the wider UNFCCC definition of grassland, which also includes shrubland; the difference is pronounced in countries with large areas of unproductive grassland (Denmark, Finland, the Baltic countries and Poland). The match with other sources is visibly better when only productive grassland is considered (Denmark, Estonia, Poland), although Latvia and Lithuania are counterexamples. Overall, the information on grassland on organic soils is less conflicting than for cropland, but strong deviations remain in some countries, including against the UNFCCC submissions (Bulgaria and Lithuania).

An alignment of the CAPRI data with other sources has not yet been undertaken, for two reasons. First, the grassland case shows that adopting absolute organic soil areas may be risky if the underlying cropland and grassland areas are not aligned as well; area shares, that is grassland on organic soils relative to total grassland, would be needed instead. Second, CAPRI also covers additional European countries and non-European regions, so an alignment would have to be achieved for all of them.

Emission coefficients

Under the EUCLIMIT-6 project, there was some information with the GLOBIOM team that led to the adoption of emission coefficients from the 2013 Wetlands supplement (Chapter 2) to the IPCC guidelines of 2006. In this respect, the models are apparently already aligned.

Rewetting cost

The current CAPRI assumption is that rewetting involves a cost of 216 Euros/ha. This is the assumed synthetic mean for a wide range of different cost amounts found in the literature by JRC staff at the time of the ECAMPA-4 study. This is also close to the GLOBIOM assumption (see below).

Even though initially envisaged, it has not been possible to collect sufficiently settled information on partial rewetting options for the whole of Europe to reflect paludiculture options that would permit continuing with some economic use of "protected" areas.

Modelling options for scenario implementation

The rewetting mitigation measure is steered in CAPRI with an implementation share defined as the rewetted area relative to the total area of organic soils used as cropland or grassland (separately). These implementation shares may be set exogenously, which was the strategy to align with IMAGE scenario work in the framework of the "comprehensive" scenarios. Alternatively it would also be possible to specify a carbon price, potentially only for emissions from histosols, to have the specification of histosol protection steered by profitability and the carbon price.

4.4.2. IMAGE

Peatland degradation and restoration are represented in the IMAGE model in terms of greenhouse gas emissions, land use patterns and the macro-level agro-economic effects of protection and restoration policies (Doelman et al., 2023). In the default setup, a peatland distribution map from Stoorvogel et al. (2014) is overlayed with endogenous land use patterns. All peatlands under agricultural land use are assumed to be degraded, while other areas are assumed to be intact. To calculate GHG emissions, emission factors from IPCC guidelines are taken for intact, degraded and rewetted peatlands and multiplied by peatland areas per category (IPCC, 2014; Wilson et al., 2016). For policies, exogenous area-based measures on peatland protection and restoration can be implemented.

For this project, we have updated the peatland distribution map for Europe using the recently published European Wetland Map (EWM) developed by the ALFAwetlands project (Tegetmeyer et al., 2025).

Figure 11 shows the changes in peatland distribution between the default IMAGE approach and the new EWM-based approach. With the new peatland map, total area in the EU increased from 205,000 km^2 to 233,000 km^2, with substantial increases in Ireland, the Netherlands, and Northwestern Germany. In northern Finland, no peatlands are present in the EWM map due to a data issue. The EWM team is working on a solution.

In the EU, degraded peatland areas increased from 43,900 km^2 to 48,200 km^2 (Figure 11). Correspondingly, emission estimates are slightly higher at 113 Mt CO_2/yr in the default setup compared to 122 Mt CO_2/yr in the updated version. The areas and emissions reported here are based on version 3 of the European Wetland Map.

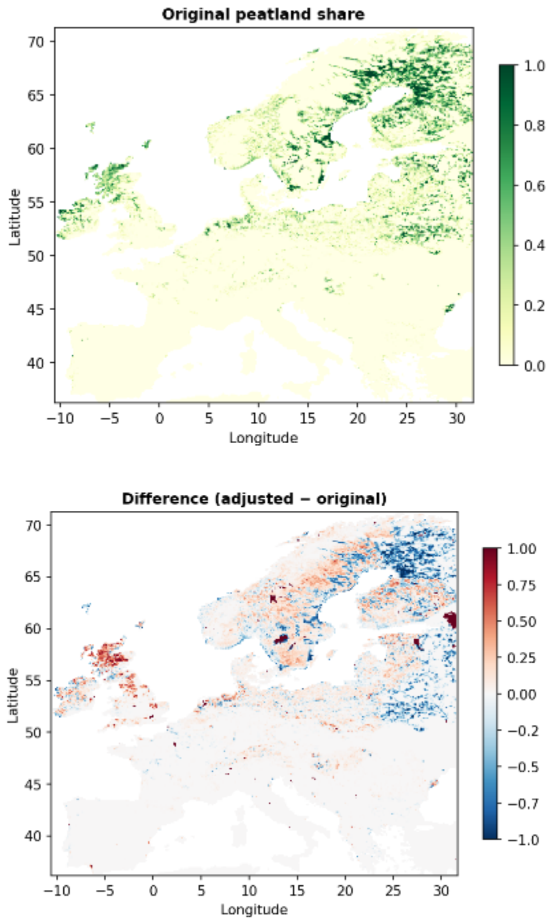

Figure 11: Peatland shares per 5 arc-min gridcell in default IMAGE setup based on Stoorvogel et al., 2014 (original peatland share), 2) updated peatland shares based on European Wetland Map (adjusted peatland fraction)

4.4.3. GLOBIOM

In GLOBIOM, peatland rewetting refers to raising the water table of drained peatland to or near the soil surface, a condition unsuitable for conventional crops and grasses. Rewetting transforms drained soils into wetlands, enhancing biodiversity and significantly reducing GHG emissions. Although rewetting decreases CO_2 and N_2O emissions by reducing soil oxidation, it can increase short-lived CH_4 emissions due to methanogenesis. Hence, accounting for all post-rewetting emissions is essential for accurate climate assessments.

Model mechanism

Rewetting in GLOBIOM can be initiated via two mechanisms. First, via an exogenously predefined restoration area target, whereby rewetting is implemented strictly to meet predetermined annual goals. Second, rewetting can occur endogenously through the application of GHG prices to emissions from drained agricultural peatlands. In this case, GHG pricing acts as an economic incentive, encouraging rewetting to reduce GHG emissions from drained peatlands.

To align with the objective of peatland protection set in the GAEC standards, the model assumes no additional peatland is drained for agricultural expansion in the EU in future years. Accordingly, the maximum area of drained agricultural peatland is capped at the 2020 level, effectively prohibiting further expansion.

Area of agricultural peatland

The area of drained agricultural peatland across Europe is derived from several sources. First, peatland distribution is identified using the European Wetland Map (EWM). Second, the Corine Land Cover (CLC) 2018 dataset is overlaid to identify cropland and grassland located on peatland, with the assumption that peatland used for agricultural production is drained. These areas are then aggregated at the LUID level, consistent with the LUM Geodatabase and implemented in GLOBIOM.

Finally, national drained peatland areas are calibrated to values reported in the UNFCCC Common Reporting Tables (CRT) from the 2025 submission. Specifically, the “Area of organic soil” reported in Table 4.B (Cropland) and 4.C (Grassland) of the CRTs is used as the national drained peatland area for each land-use type.

Emission factors for drained and rewetted peatland

Net GHG mitigation from rewetting is computed as the avoided emissions from drained peatland minus the additional emissions from rewetted peatland. Both components are estimated by multiplying the respective emission factors by the rewetted area.

Emission factors for CO_2 and N_2O from drained peatland are extracted from the UNFCCC CRTs. CO_2 emissions from drained peatland are retrieved from the "Net carbon stock change in soils" reported in Table 4.B and 4.C (in kt C) and from “CO_2 EMISSIONS” in Table4(II; in ktCO_2). Total CO_2 emissions from peatlands are calculated by converting the "Net carbon stock change in soils" data into “kt CO_2” and aggregating them with the reported “CO_2 EMISSIONS”. Emission factors for extracted CO_2 values from peatland are then derived by dividing total CO_2 emissions by the nationally reported organic soil area of Cropland or Grassland in the unit of “tCO_2 ha-1”.

Similarly, N_2O emission factors are derived using N_2O emissions (in kt) reported in Table 3.D and the corresponding national organic soil areas from the 2025 CRTs. CH_4 emission factors for drained peatland are not consistently reported across countries' CRTs. Therefore, to ensure data completeness, CH_4 emission factors for drained peatland are taken from Wilson et al. (2016).

Emission factors for all GHGs from rewetted peatland are also retrieved from Wilson et al. (2016) for both cropland and grassland. For rewetted grassland, emission factors for different nutrient statuses are assigned to EU countries using Martin and Couwenberg (2021). For countries lacking nutrient status information, drained grassland is assumed to be nutrient-rich in temperate climate zones, consistent with the IPCC Tier 1 approach (Hiraishi et al., 2014), and the corresponding emission factors are applied.

All peatland GHG fluxes are converted to CO_2 equivalents using a 100-year global warming potential (GWP) timescale, including climate-carbon feedbacks, as reported in the IPCC Fifth Assessment Report (AR5) (IPCC, 2014).

Rewetting cost

Based on the LAMASUS costing database, an average investment cost of approximately 205 USD ha-1 yr-1, which is converted from 3,262 EUR ha-1 using a 3% interest rate over 30 years, is applied across all EU27 countries within a quadratic cost function. Opportunity costs from foregone agricultural production are modelled endogenously within GLOBIOM.

5. Integration of econometric parameters from WP4 models

This chapter documents how the econometric parameters estimated in WP4 are integrated into the macro-level models. Two sets of parameters are covered. The first are technical yield shifters: crop- and country-specific trajectories of technological change, estimated in a multilevel Bayesian panel regression of crop yields on real GDP per capita and projected to 2100 under the SSP scenarios (Section 5.1). The second are improved land-use change parameters for GLOBIOM: agricultural land supply elasticities and land-use transition parameters, estimated from observed European land-cover transitions in a spatial multinomial choice framework (Section 5.2). For both, the chapter describes the underlying data, the estimation approach, and how the resulting estimates are translated into model parameters; Section 5.2.1 documents downscalepy, the Python implementation used to apply the estimated transition parameters at grid level.

5.1. TECHNICAL YIELD SHIFTERS

The methodology for generating crop yield shifters of *technological change* follows a multi-step process that integrates econometric modelling with Shared Socioeconomic Pathways (SSP) projections. This framework produces robust estimates of crop yield changes by aligning quantitative models with the broader socioeconomic assumptions of the SSP framework. This chapter details the data sources, model specifications, and projection approach used to operationalize these pathways.

5.1.1. Data and model specification

The process begins with the compilation of historical data and future projections from authoritative sources. The historical sample span for model estimation ranges from 1971 to 2015, with all data on crop yield, harvested area, and socioeconomic indicators like RGDPPC (Real Gross Domestic Product per Capita) sourced from the FAOSTAT database. For future projections, the model uses scenarios for RGDPPC from the SSPs, specifically from the IIASA SSP Scenario Database, which provide country-level population & GDP projections up to the year 2100.

The econometric model is a multilevel Bayesian linear regression, which is estimated separately for each crop. This key feature acknowledges that the relationship between socioeconomic drivers and yield is unique to each crop. In total, the analysis represents 152 countries, although the specific number of countries included in each crop model varies between 35 and 125, depending on data availability. For each crop-specific model, the relationship between yield and the main driver is formulated as a panel regression over time:

$$YIELD_{j,t} = \beta_{0,j} + \beta_{1,j} \cdot ln\left(RGDPPC_{j,t}\right) + \epsilon_{j,t},$$

with

$$\epsilon_{j,t} \sim Student's\ t(\nu, 0, \sigma \cdot w_{j,t}).$$

Here, $YIELD_{j,t}$ represents the crop yield in levels (*t/ha*) for region *j* at time *t*. The main predictor is the natural logarithm of contemporaneous, region-level *RGDPPC*, $ln\,(RGDPPC_{j,t})$, which allows the model to capture a non-linear relationship where the impact of changes in RGDPPC diminishes as an economy develops. The error term $\epsilon_{j,t}$ is assumed to follow a *Student's t-distribution*, making the model robust to outliers.

The coefficients $\beta_{0,j}$ (intercept) and $\beta_{1,j}$ (RGDPPC elasticity) are modeled hierarchically. Each is defined as a sum of a global pooled effect and a region-specific deviation:

$$\beta_{k,j} = \beta_k^{pool} + \beta_{k,j}^{reg}$$

where *k* refers to the intercept (*k=0*) or log-RGDPPC coefficient (*k=1*). The regional deviations, $\beta_{k,j}^{reg}$, are treated as random effects drawn from a normal distribution, with their variances estimated from the data. This hierarchical structure allows the model to benefit from information across all regions while also accounting for regional characteristics. The estimation is carried out using a non-centred parameterisation to ensure efficient MCMC sampling.

A crucial aspect of the model is the *prior error variance*, which is weighted to give more importance to recent data points. This is done by specifying the variance of the error term as $\sigma \cdot w_{j,t}$ where $w_{j,t}$ is a weighting factor that increases for more recent observations. This ensures that the model's coefficients are more reflective of the most current trends in yield and socioeconomic development.

5.1.2. Yield projection methodology

The yield projections are constructed in an iterative, step-by-step process. Once the model's coefficients are estimated (as described above), they are used to advance the yield from a base year into the future, using scenarios from the SSPs. For a given SSP scenario, the fundamental formula for calculating the projected yield per crop type *i* and region *j* is:

$$Projected\ Yield_{i,t+1}^{SSP} = Projected\ Yield_{i,t}^{SSP} + \Delta Yield_{i,t+1}^{SSP}.$$

The change in yield over a single 5-year time step (*t+1*), $\Delta Yield_{i,t+1}^{SSP}$, is driven by the change in the main predictor, RGDPPC, as provided by the SSP scenarios:

$$\Delta Yield_{i,j,t+1}^{SSP} = \hat{\beta}_{1,i,j} \cdot \left[ln\,(RGDPPC)_{j,t+1}^{SSP} - ln\,(RGDPPC)_{j,t}^{SSP}\right].$$

Here, $\hat{\beta}_{1,i,j}$ is the estimated coefficient for the log-RGDPPC variable for a specific region (*j*). The superscript *SSP* is added to indicate that the projected yield and the RGDPPC values are specific to a particular SSP scenario.

This iterative calculation is subject to two critical constraints to ensure the projections are physically plausible:

1. Lower Bound: If the calculated $\Delta Yield_{i,j,t+1}^{SSP}$ is negative, it is replaced with the lowest positive projected change across countries in the same timestep. This prevents the model from projecting yield declines in the absence of other specified negative factors.
2. Upper Bound: As the Projected Yield approaches a predefined maximum limit (a multiple of historically high yields), a *dampening function* is applied. This function gradually reduces the magnitude of $\Delta Yield_{i,j,t+1}^{SSP}$, ensuring the projections do not grow indefinitely and remain within a realistic range.

Finally, the projected yield is used to calculate the technical yield shifter, defined as the ratio of the projected yield to the yield in the base year (2000). This produces a unitless factor, allowing for straightforward comparison across regions and crop types.

Figure 12 illustrates the technical yield shifters for the crop "Wheat", showing how they vary across five countries chosen to span Northern, Western, Southern, Central and Eastern Europe, and all SSP scenarios.

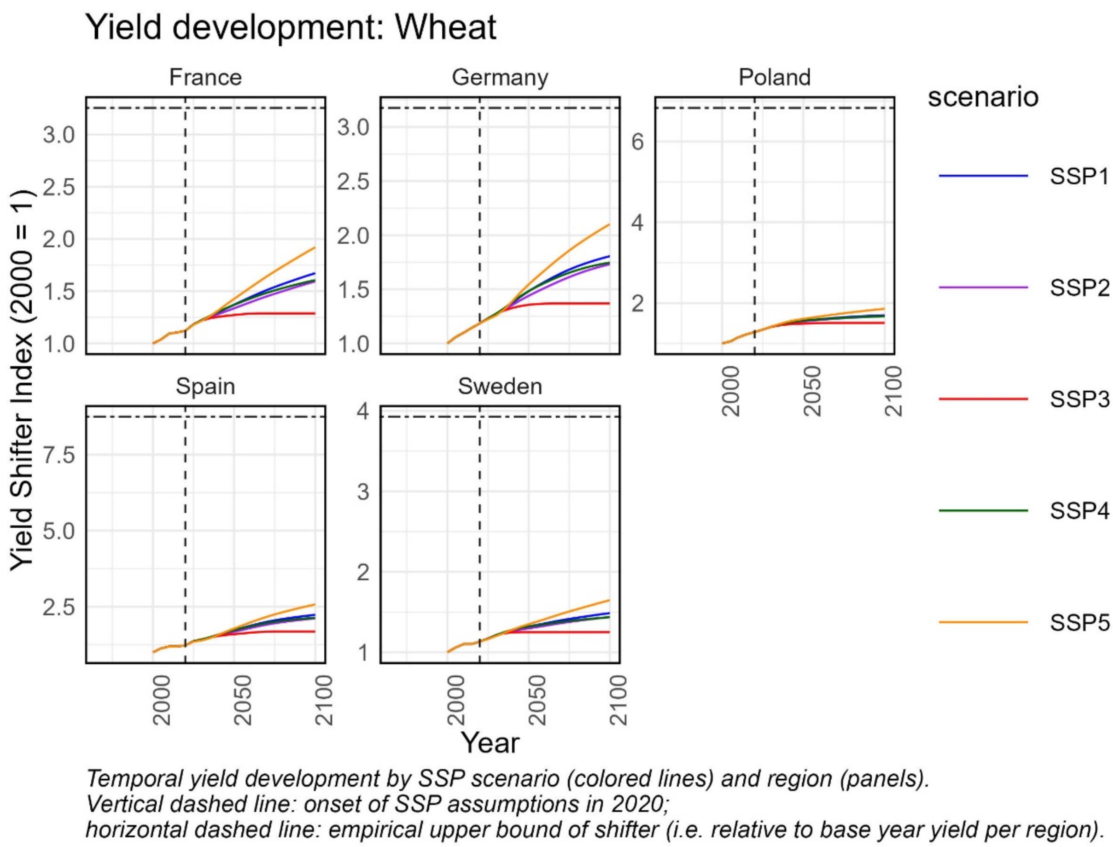

Figure 12: Wheat yield shifter trajectories for selected countries and all SSP scenarios

5.2. IMPROVED LAND-USE CHANGE PARAMETERS

Historically, land-use change has been a continuous socio-ecological process, constantly evolving to meet the shifting demands of human development. On a global scale, this dynamic trajectory continues today: land remains a highly contested resource, shifting rapidly in response to population growth, changing dietary preferences, and the transition toward a bio-based economy. The European Union, however, presents a distinctly different context. In contrast to these global trends of agricultural and urban expansion, land-use change (LUC) dynamics within the EU are relatively stagnant. The European land base is already highly saturated and heavily mediated by rigid institutional frameworks, legacy agricultural policies, and established conservation mandates. In this highly regulated environment, where the physical expansion of agricultural land is fundamentally constrained, understanding how land allocation practically responds to underlying market signals remains a critical research objective.

Quantifying the causal drivers of land-use change presents significant econometric challenges. As highlighted in a recent perspective on empirical land-use modelling (Eigenbrod et al., 2026), land-use decisions are not simple mechanical outcomes, but rather emergent properties of complex socio-ecological systems. More specifically, they result from interconnected processes driven by heterogeneous economic agents operating under complex biophysical, market, and regulatory constraints. Accurately estimating the parameters of these drivers requires overcoming several general methodological hurdles, including severe endogeneity, unobserved confounding variables, and the inherent spatial dynamics of immobile land. Relying on purely correlational analyses in this context risks yielding biased parameter estimates, ultimately leading to suboptimal or misleading policy design.

In this deliverable, we ground these overarching econometric challenges in a pertinent empirical application: the estimation of agricultural land supply elasticities. Quantifying how regional land allocation responds to economic incentives—specifically, fluctuations in agricultural land rents—serves a useful function beyond the immediate econometric exercise. We provide empirical estimates that are valuable for cross-checking and calibrating the structural parameters that dictate land-use responsiveness in macroeconomic equilibrium models. By modelling the relationship between European land constraints and market forces, we help ensure that the large-scale integrated models used for policy assessment are supported by empirically grounded behavioural dynamics.

To systematically address the socio-ecological complexities outlined by Eigenbrod et al., we employ an empirical strategy of increasing model complexity. By progressively building up the econometric framework, we demonstrate how to tackle the specific hurdles inherent in estimating causal land supply elasticities in the highly saturated EU environment:

- **Endogeneity and Confounding Variables:** Isolating the true causal effect of agricultural land rents from correlational data is a primary challenge. Local land-use decisions are simultaneously influenced by global commodity prices, regional subsidies, and localized regulations. As we increase model complexity, we deploy techniques that effectively control for these endogeneity issues.

- Spatial Dynamics: Land is physically immobile, requiring us to move beyond standard assumptions of independence. Our advanced specifications account for spatial heterogeneity (e.g., variations in soil quality and climate) and spatial spillovers, where the rent, use, or conservation status of one plot affects the economic viability of neighboring areas.
- Asymmetries and Rigidities: Because the EU land matrix is heavily regulated, we observe that supply responses to land rents tend to be asymmetric. Expanding agricultural land is often structurally difficult or legally restricted, while contraction is mediated by sunk costs and legacy policies. Consequently, standard linear models are insufficient, necessitating more complex, non-linear approaches to capture true market dynamics.

By systematically advancing through these layers of model complexity, we aim to provide a robust framework for estimating agricultural land supply elasticities. Accurately capturing this response to agricultural land rents provides the necessary quantitative "plug" for large-scale economic and integrated assessment models, ensuring they rely on sound structural parameters to evaluate environmental and climate policies in a constrained landscape.

5.2.1. Stylised framework and empirical proxies

In a standard partial equilibrium framework, agricultural land supply is conceptually straightforward: we can visualize it as a classic supply curve mapping the total quantity of allocated land (the horizontal axis) against its prevailing market rent (the vertical axis). Theoretically, estimating the elasticity of this curve—how structurally responsive the land matrix is to price signals—requires observing continuous, localized intersections of land supply and demand across space and time. Formally, we require matched panel data to trace the function $L_{it} = f(R_{it})$, where L is the land allocated and R is the rent at location i in year t.

However, a defining stylised fact of empirical macro-spatial modelling is that these perfect, localized (L, R) coordinates are rarely observable at a continental scale. Rather than observing continuous, parcel-level bid-rent functions, we are empirically constrained to observing discrete, aggregated spatial footprints and regionalized price averages.

To empirically trace out this aggregate supply curve and bridge the gap between theoretical micro-foundations and observable macro-dynamics, we operationalize our spatial panel using the following proxies:

$\boldsymbol{L}$ - Land supply is proxied by the physical quantity of land allocated to agriculture, taken from the CORINE land cover accounting layer. Drawing on annual time-series remote sensing data from 2000 to 2018 via the LAMASUS LUM geodatabase, this captures the discrete spatial footprint and the structural rigidities of the European land matrix over time.

R – Land rent is proxied by a NUTS-level agricultural land rents dataset derived from the Farm Accountancy Data Network (FADN) and provided by the LAMASUS project. These aggregated regional values serve as the exogenous variation representing the economic returns to, and opportunity costs of, maintaining agricultural land.

To properly operationalize the land supply variable within this econometric framework, we cannot merely track the existing agricultural footprint. Estimating how supply expands or contracts in response to rent fluctuations inherently requires us to model the extensive margin—the boundary where agricultural and non-agricultural land uses compete. Therefore, processing the remote sensing data requires us to take two distinct classification steps.

First, we define the active agricultural land base. This involves categorizing and aggregating the relevant CORINE land cover classes—such as arable land, permanent crops, pastures, and heterogeneous agricultural areas—into a unified agricultural footprint for each regional unit over the time series. This provides our empirical baseline for ***L***.

Second, and more critically for estimating a realistic supply elasticity, we define the pool of land that could, in theory, be transformed into agricultural use. Because the European land base is highly saturated, we assume agricultural expansion cannot occur in a vacuum; an increase in agricultural land must systematically displace another land cover. Rather than relying on theoretical assumptions about biophysical suitability, we home in on potential agricultural land by identifying classes based on empirically observed transitions at the pixel level. By rigorously tracking actual land-cover changes both flowing *into* agriculture and flowing *out* of agriculture between the years 2000 and 2018, we empirically isolate the specific non-agricultural classes (e.g., specific transitional woodlands or natural grasslands) that demonstrably participate in the margin of agricultural expansion and abandonment.

Figure 13 provides a visual summary of the empirical inflows into agriculture. Panel A illustrates the total EU-wide magnitude of land transitions into four primary agricultural classes from non-agricultural source categories. As the bar charts indicate, agricultural expansion is highly concentrated, drawing primarily from a distinct subset of classes such as transitional woodland-shrubs, natural grasslands, and coniferous forests. Panel B demonstrates the spatial heterogeneity of these shifts across Member States, revealing that the margin of expansion is highly localized in countries like Spain, Finland, and Portugal. Concurrently, the analogous land outflows from agriculture—which similarly determine the active margin of land abandonment and further define our potential land pool—are detailed in Annex 8.1.

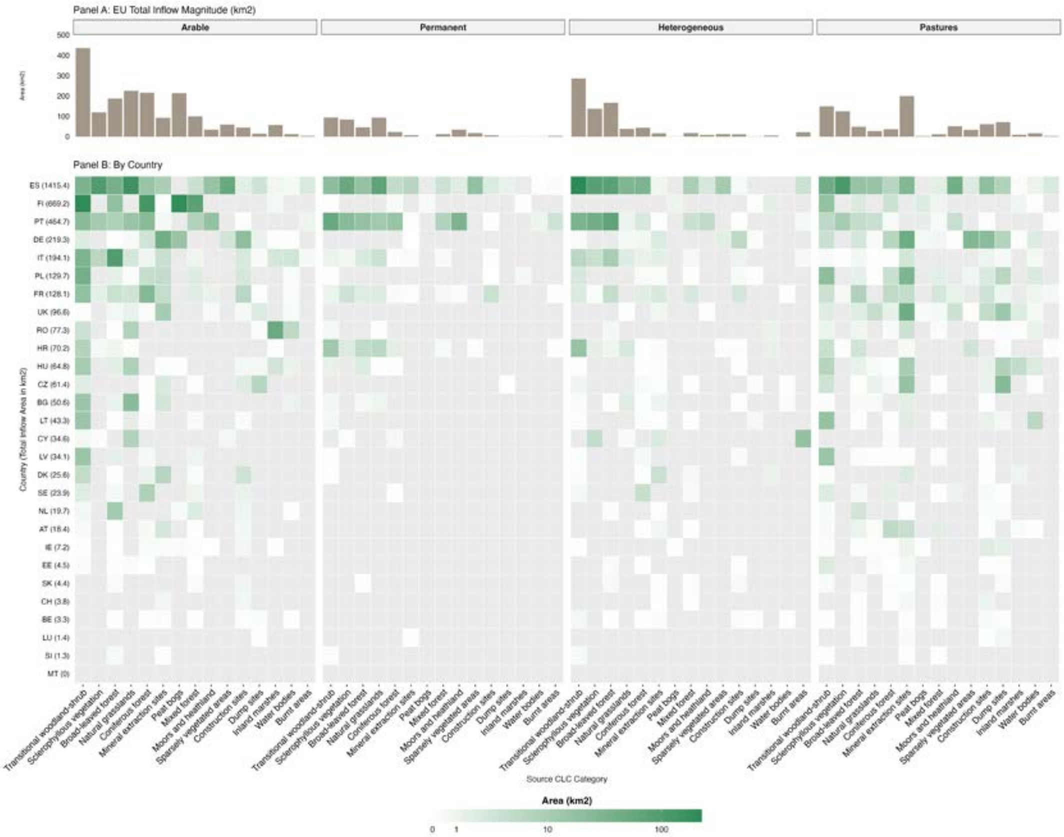

Figure 13: Empirically observed land-cover transitions to agricultural use across the EU (2000–2018).

Note: Panel A (top) displays the total EU-wide magnitude of land inflows (in km²) into four primary agricultural classes from non-agricultural CORINE Land Cover (CLC) categories. Panel B (bottom) provides a country-level breakdown of these inflows via a heatmap, highlighting the pronounced spatial heterogeneity of agricultural expansion sources.

By utilising this empirical transition matrix, we inherently resolve the issue of masking out inaccessible land. As corroborated by the pervasive white gaps (zero values) across multiple source categories in Figure 13, Panel B, parcels categorised as established urban fabrics, major infrastructure, water bodies, or high-elevation bare rock naturally exhibit zero transition probability to agriculture within our observed 2000 to 2018 pixel data, seamlessly excluding them from our potential land pool.

To map these pixel-level dynamics onto our economic framework, we must address spatial scaling. Because our exogenous price signal—the agricultural rent dataset—is provided at the NUTS2 regional level, we aggregate our high-resolution land-use classifications to match this resolution. Consequently, our dependent variable (L) is formally expressed as the share of active agricultural land relative to the total potential agricultural area within each NUTS2 region. Structuring the spatial panel around this empirically bounded, aggregated share ensures that our estimated elasticities reflect true, constrained responsiveness rather than assuming a frictionless land frontier.

Figure 14 visualises the core empirical relationship at the heart of our spatial panel. By plotting the agricultural rent against the active agricultural land share for each NUTS2 region, the scatter plot empirically approximates our aggregate supply curve framework ($L_{it} = f(R_{it})$). The lines connecting the annual observations trace the distinct temporal trajectory of each region between 2000 and 2018. While localised pixel-level transitions constantly occur (as seen in Figure 13), the relatively constrained horizontal movements of the regional trajectories in Figure 14 highlight the overarching stability and structural rigidity of the regional land matrix. Even amid significant vertical fluctuations in land rents, the land shares shift slowly. Understanding and causally estimating the underlying responsiveness of these rigid, aggregated shares to fluctuating regional rents forms the core analytical task of the subsequent econometric models.

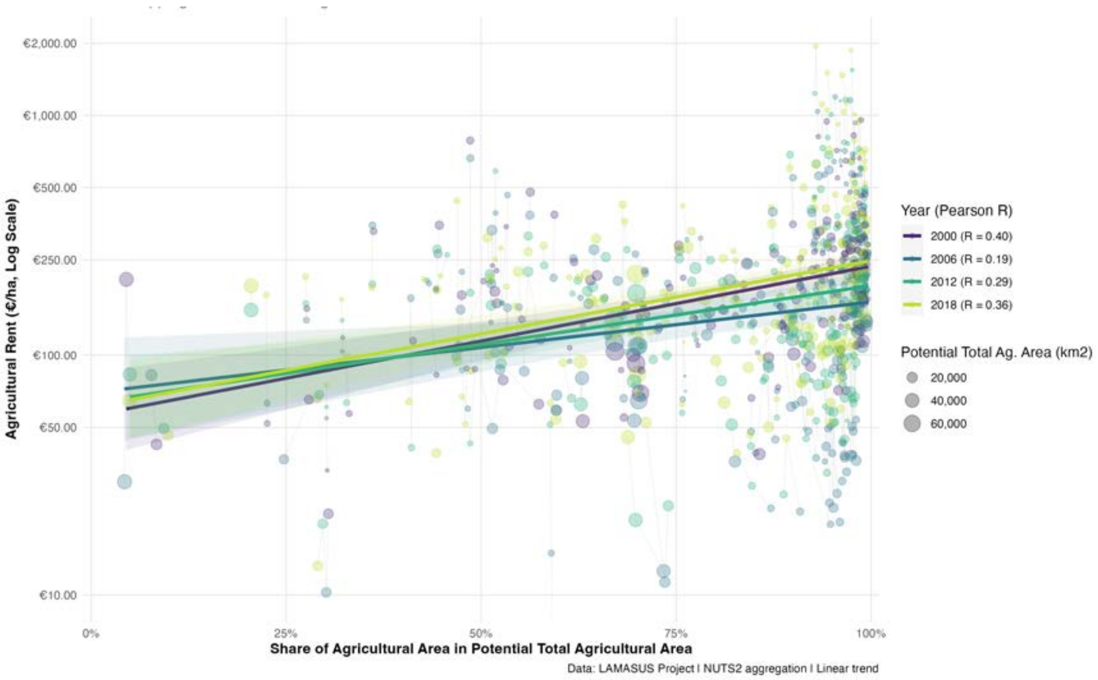

Figure 14: Descriptive scatter plot of agricultural land rents versus agricultural land shares across EU NUTS2 regions (2000–2018).

Note: The y-axis displays the regional agricultural rent (R), while the x-axis represents the share of active agricultural land within the total potential area (L). Observations for each NUTS2 region are connected by lines to trace their temporal trajectories, with point sizes indicating the total potential area of the respective region.

5.2.2. Econometric framework: the multinomial choice model

While our empirical data are observed as aggregated land shares at the regional level, the theoretical foundation of our econometric specification is fundamentally rooted in a microeconomic discrete choice framework. To formalise the causal drivers of land-use allocation and estimate the associated supply elasticities, we build our analysis upon a Multinomial Logit (MNL) model. This structural approach allows us to mathematically represent the decision-making process of representative economic agents operating within the constrained European land base.

Building on the empirical proxies defined in Section 2, we map our observed exogenous price signal—agricultural rent (R)—into the utility function that dictates the resulting land supply (L). The standard MNL model assumes that the utility a landowner i derives in time t from choosing a specific land-use alternative j (from a finite set of J possible, mutually exclusive alternatives within our potential land pool) is composed of a deterministic, observable component and a random, unobservable error component.

To isolate the causal effect of market incentives in this estimation, we model the deterministic utility as a function of agricultural rent while controlling for a vector of observable confounding factors and other structural drivers. Formally, the underlying utility equation is specified as:

$$U_{ijt} = V_{ijt} + \varepsilon_{ijt} = \alpha_j + \gamma_j R_{it} + \beta_j X_{it} + \varepsilon_{ijt}$$

where:

- U_{ijt} is the latent (unobserved) total utility that landowner i receives from selecting land-use alternative j at time t.
- V_{ijt} represents the deterministic portion of the utility.
- α_j is the alternative-specific intercept for land use j, capturing the baseline, intrinsic preferences or average structural rigidities associated with maintaining that specific land cover.
- R_{it} is our primary variable of interest: the expected agricultural land rent in region i at time t.
- γ_j is the alternative-specific parameter capturing the causal responsiveness (utility weight) of land-use j to fluctuations in agricultural rent.
- X_{it} represents a vector of observable confounding factors or other regional drivers (such as biophysical & topographical characteristics, climate indices, or socio-economic variables) for region i at time t that simultaneously influence land-use decisions.
- β_j is the vector of alternative-specific coefficients corresponding to these confounding variables, capturing how each factor shifts the utility of choosing land-use j.
- ε_{ijt} is the stochastic error term, capturing unobserved, idiosyncratic factors and individual constraints affecting the choice.

Assuming the error terms ε_{ijt} are independent and identically distributed (i.i.d.) following a Type I Extreme Value distribution, the individual probability P_{ijt} of choosing alternative j takes the standard logistic form: $P_{ijt} = \frac{\exp(\alpha_j + \gamma_j R_{it} + \beta_j X_{it})}{\sum_{k=1}^{J} \exp(\alpha_k + \gamma_k R_{it} + \beta_j X_{it})}$

While this structural framework fundamentally describes parcel-level decisions, our current empirical strategy estimates these dynamics at the NUTS2 scale. We operationalise this by treating the observed land allocations as a discrete count process, entering land-cover data as integer counts of spatial units (hectares) rather than continuous proportions.

Let Y_{ijt} denote the absolute area allocated to category j in region i at time t, out of a total regional land pool $N_{it} = \sum_{k=0}^{J} Y_{ikt}$. The joint distribution of these counts follows a multinomial distribution:

$$\left(Y_{i0t}, Y_{i1t}, \dots, Y_{iJt}\right) \sim \text{Multinomial}\left(N_{it}, P_{i0t}, P_{i1t}, \dots, P_{iJt}\right)$$

By structuring the data as multinomial area counts, our Bayesian estimation naturally weights each region by its total physical area (N_{it}). Consequently, physically larger regions contribute proportionally more discrete choice points to the model. This ensures our estimated market responses and covariates are realistically driven by the regions holding the vast majority of Europe's land mass, rather than treating small and large administrative units as equally influential.

Ultimately, this count-based formulation links the structural micro-probabilities (P_{ijt}) directly to our empirically observed regional land shares, calculated as $s_{ijt} = Y_{ijt}/N_{it}$. In our analysis, the share allocated specifically to active agriculture serves as our primary land supply variable (L_{it}).

The Baseline Pooled Model

In line with our empirical strategy of progressively increasing model complexity to handle socio-ecological endogeneity, the first model we estimate is a simple pooled multinomial logit model.

In this initial specification, we treat the panel data as a single cross-section over time, pooling all observations across NUTS2 regions and years. This naive baseline model assumes that all regions share the same underlying parameters and that observations are completely independent of one another.

To estimate this relationship using our aggregated regional shares (s_{ijt}), we apply the standard log-odds transformation to the non-linear probability function. By defining a baseline outside land-use category $j = 0$ (in our case, the pool of uncultivated potential agricultural land), we normalise its parameters to zero ($\alpha_0 = 0$ and $\gamma_0 = 0$) to achieve model identification. The model can then be linearised into our baseline estimation equation:

$$\ln\left(\frac{s_{ijt}}{s_{i0t}}\right) = \alpha_j' + \gamma_j' R_{it} + \nu_{ijt}$$

where:

- $\ln\left(\frac{s_{ijt}}{s_{i0t}}\right)$ is the log-odds ratio of the share of land in use j relative to the baseline non-agricultural potential land pool.
- $\alpha_j' = \alpha_j - \alpha_0$ is the relative alternative-specific intercept.

- $\gamma'_j = \gamma_j - \gamma_0$ captures the relative effect of agricultural rents on transitioning land into (or keeping land in) category j versus the baseline pool.
- ν_{ijt} represents the composite aggregate error term.

By starting here, we establish a foundational elasticity estimate driven strictly by the contemporaneous variation in the rent variable (R_{it}). However, this simple pooled specification assumes that the aggregate error term ν_{ijt} is entirely uncorrelated with the rent variable—a highly restrictive assumption given the institutional realities of the European land matrix. The estimated elasticities are reported in Table 9. The associated pooled land-supply curves in Figure 15 show for these four land use categories the share of land by agricultural rent in Euro per hectares.

Table 9: Estimated land supply elasticities by land-use category

CATEGORY	MEAN	Q2.5	Q97.5
Arable	0.579	0.577	0.581
Permanent	0.531	0.527	0.535
Heterogeneous	0.346	0.343	0.349
Pasture	0.656	0.653	0.659

Note: Mean and 2.5th / 97.5th percentiles of the posterior distribution.

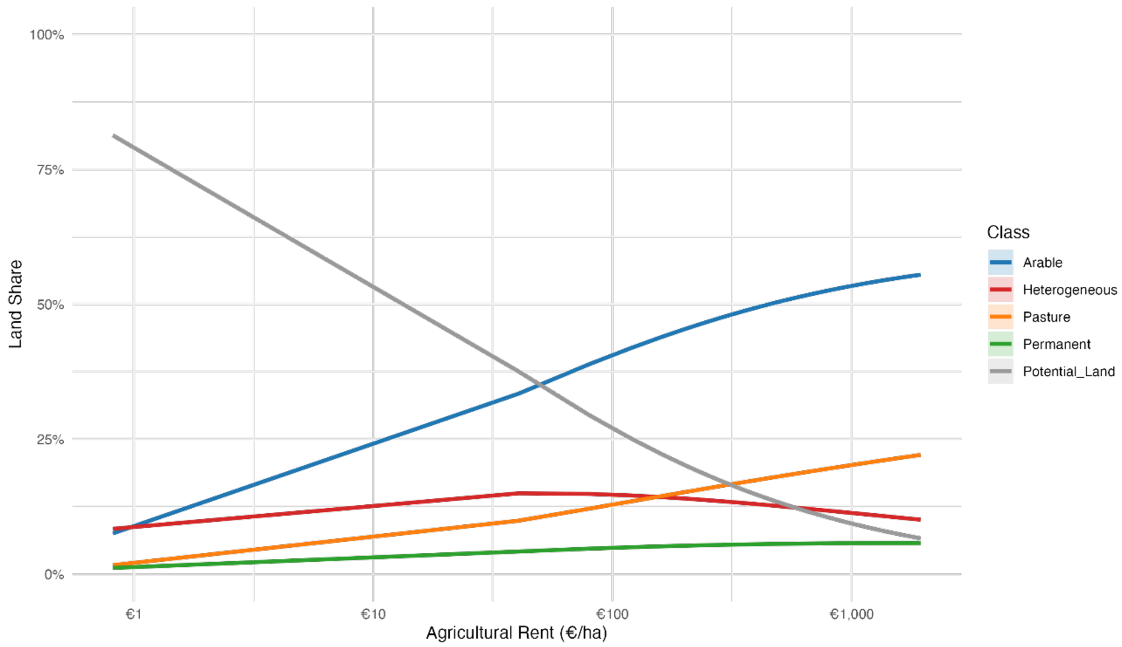

Figure 15: Pooled land supply curves by land-use class, NUTS2 regions

The Country-Level Multilevel Model

To address the limitations of the pooled model, our second iteration introduces a multilevel (hierarchical) structure.

The pooled model assumes that agricultural land responds to rent fluctuations identically across the entire continent. However, land-use decisions within the EU are inherently nested. NUTS2 regions operate within the specific institutional and regulatory boundaries of their respective Member States. While the EU shares an overarching Common Agricultural Policy (CAP), the domestic implementation of these policies, along with national conservation mandates and distinct agricultural labour markets, creates significant country-level heterogeneity.

To capture this hierarchical data structure, we extend our baseline specification into a multilevel mixed-effects model. We introduce country-level random effects for both the baseline land allocation (a random intercept) and the behavioural responsiveness to market incentives (a random slope for agricultural rent).

Letting c denote the specific country in which the NUTS2 region i is located, the log-odds of choosing land-use alternative j relative to the baseline potential land pool ($j = 0$) is modelled compactly as:

$$\ln\left(\frac{s_{ijt}}{s_{i0t}}\right) = (\alpha_j + \alpha_{jc}) + (\gamma_j + \gamma_{jc})R_{it} + \epsilon_{ijt}$$

where:

- α_j and γ_j are the *hierarchical pooled effects*, representing the average, EU-wide baseline preference and the aggregate supply response (elasticity parameter) to agricultural rents for land-use alternative j.
- α_{jc} and γ_{jc} are the *country-specific random effects* (intercept and slope, respectively), typically assumed to follow a joint multivariate normal distribution. They capture how country c's baseline allocation and rent sensitivity structurally deviate from the EU average.
- ϵ_{ijt} is now the remaining idiosyncratic regional error term.

By allowing both the baseline land allocation and the marginal effect of agricultural rent to vary by country, this multilevel specification directly addresses the unobserved spatial and institutional heterogeneity inherent in the European land base. Although European agriculture operates under the shared umbrella of the CAP, land markets remain deeply embedded in national contexts—filtered through country-specific legal frameworks, zoning regulations, and historical subsidy legacies. A standard pooled model forces a single, uniform elasticity across all regions, risking severely biased estimates by conflating these unobserved structural differences with true price responsiveness. By separating these dynamics, the random intercepts (α_{jc}) control for the unobserved country-specific factors that dictate overall agricultural footprints, while the random slopes (γ_{jc}) allow the supply elasticity to flexibly reflect varying national market rigidities. This structural flexibility ensures that our aggregate, EU-wide elasticity estimate (γ_j) is robustly isolated from country-level institutional noise.

5.2.3. downscalepy: a Python implementation of the MNL bias-correction solver for land-use downscaling

The *downscalr* package comprises two distinct modules: a Prior module, which estimates pixel-level land use transition probabilities using a Bayesian MNL regression model fitted to observed land use change data and explanatory covariates; and a Downscale module, which takes those prior probabilities — from whatever source — and applies a bias correction to ensure that the spatially aggregated allocation is consistent with prescribed aggregate area targets. *downscalepy*[ii] implements the Downscale module exclusively. It is agnostic about how the prior probabilities were generated and imposes no requirement on the Prior module. This separation of concerns is an intentional design choice: the bias correction step is a self-contained spatial accounting problem, independent of the econometric or predictive model used upstream. The module has been developed and tested in the context of JRC land use modelling work.

The solver is grounded in the Multinomial Logit (MNL) framework for discrete choice modelling (McFadden, 1974), as applied to land use change modelling by Krisztin et al. The fundamental problem is one of constrained spatial allocation: given prior transition probabilities or land use suitability at the pixel level and prescribed aggregate area targets at the regional level, find a spatially consistent allocation that minimises the discrepancy between simulated and target areas while respecting transition constraints.

Mathematical formulation

For each pixel i and land-use class j, the allocation is defined as:

$$z_{ij} = \mu_{ij} = (x_j \cdot p_{ij}) / \Sigma_k (x_k \cdot p_{ik})$$

where:

- z_{ij} is the allocated share of pixel i to land-use class j
- μ_{ij} is the allocation probability (normalised share)
- x_j is the class-specific scaling factor (calibrated variable)
- p_{ij} is the prior suitability for pixel i and class j
- k indexes all land-use classes

By construction, allocations are normalised for each pixel, such that the sum of shares across all land-use classes equals one.

The total allocated area for each class j is obtained by aggregating across pixels:

$$A_j = \Sigma_i (z_{ij} \cdot a_i)$$

where a_i denotes the area of pixel i.

[ii] GitHub - anabrs1/downscalepy · GitHub

The scaling factors x_j are estimated by minimising the squared discrepancy between allocated areas and predefined target demands:

$$min\ \Sigma_j\ (\ \Sigma_i\ (z_{ij} \cdot a_i) - T_j\ )^2$$

where T_j represents the target area for land-use class *j*. The optimisation is subject to non-negativity constraints ($x_j \geq 0$ for all j).

Additionally, binary transition restrictions can be applied at the pixel level to prohibit specific land-use transitions.

Architecture

downscalepy is structured as a modular Python package (Python 3.8+), organised into four functional layers: The package structure is summarised in Table 10.

Table 10: Structure of the downscalepy package

MODULE	SUBMODULES	DESCRIPTION
core/	solver.py, mnl_functions.py, optimization.py, grid_search.py	MNL probability calculations, optimisation framework, convergence logic and fallback strategies
data/	path_detector.py, data_loader.py, validators.py, preprocessor.py	Automatic input detection, multi-format loading (CSV, Parquet, JSON), data validation and preprocessing
output/	projector.py	Generation of projection maps with full geospatial metadata; export to Parquet, CSV, and JSON formats
utils/	config.py, logger.py, performance.py	Configuration management (YAML/JSON), structured logging, memory and execution-time monitoring

The entry point is scripts/bias_correction_solver/main.py, which orchestrates the full pipeline: input detection, data loading and validation, solver execution, and output generation. The module supports both command-line invocation and programmatic use through its public API.

Input requirements

The solver expects four types of input, located in a scenario directory: The required inputs are listed in Table 11.

Table 11: Input requirements of the downscalepy solver

INPUT	FORMAT	REQUIRED COLUMNS	DESCRIPTION
Areas	CSV	ns, lu.from, value	Current land use composition per pixel; area in hectares
Priors	Parquet or CSV	ns, lu.to, value	Prior transition probabilities per pixel and target class (0–1)
Targets	CSV	lu.from, lu.to, value	Aggregate area targets by source and destination class; area in hectares

Restrictions	CSV + JSON (optional)	ns, lu.from, lu.to, value	Binary constraints on pixel-level transitions (0 = allowed, 1 = forbidden)

Optimisation strategy and robustness

A core design objective is the convergence across heterogeneous regional contexts, including areas with high class imbalance, sparse land use classes, or complex transition matrices. The module implements a cascading optimisation strategy that automatically falls back to progressively more robust methods if convergence is not achieved:

- L-BFGS-B: primary solver; a quasi-Newton gradient-based method using analytical gradients. Fast and accurate for well-conditioned problems
- SLSQP: first fallback; an alternative gradient-based constrained optimisation method
- Powell: second fallback; a derivative-free method suited to irregular objective surfaces
- Grid search: final fallback (separate module); a systematic scan over the scaling factor space, ensuring convergence for numerically difficult cases

6. Conclusion and next steps

This deliverable has documented the extension of the LAMASUS macro-level models under Tasks 7.1 and 7.2. Organic farming and grassland management are now represented explicitly in CAPRI and GLOBIOM, with their own yields, costs and emission factors. Climate-smart forest management systems have been implemented in G4M, and the forestry representation of MAGNET has been extended to harvested wood products, the paper and pulp sector and the competition for land between forestry and agriculture. Peatland rewetting has been implemented or refined as a distinct mitigation option in CAPRI, GLOBIOM and IMAGE.

We also strengthened the empirical basis of the models. Each model now takes up the historic land-use and management information of the LUM geodatabase at its highest feasible spatial resolution; the CAP Strategic Plans are encoded intervention by intervention in the CAPRI premium module and passed on to GLOBIOM and MAGNET; and the econometric estimates from WP4 enter the models as technical yield shifters and as land-use change parameters. Policy instruments that act through management requirements—eco-schemes, agri-environmental commitments, grassland extensification, rewetting of drained organic soils and changes in harvesting regimes—can therefore be simulated as management choices that respond to the policy signal, within limits derived from observed land-use change. Two qualifications apply: the uptake of the LUM geodatabase differs across models, reflecting their native resolution and data architecture, and some parameterisations still rest on interim data that will be replaced once the final estimates become available.

Building on the model developments presented in this deliverable, the harmonised baseline and the policy scenarios that use these management options and behavioural parameters are developed in work package 8 (D8.1, D8.2). In parallel, Task 7.3 completes the cross-scale integration between the macro-level models and the high-resolution modelling layer (D7.2). Parameterisations that are superseded by final data will be updated in the WP8 simulations.

7. References

Angileri, V., Guerrero, I. and F. Weiss, 2024, A classification scheme based on farming practices: A tool for labelling interventions with environmental and climate-related commitments in Common Agricultural Policy strategic plans, Publications Office of the European Union, Luxembourg, JRC133862. https://doi.org/10.2760/33560

Araujo Enciso, S. R., Perez Dominguez, I., Santini, F., Helaine, S., Dillen, K., Gay, S. H. and P. Charlebois, 2015, Documentation of the European Commission's EU module of the Aglink-Cosimo modelling system, JRC Science and Policy Reports EUR 27138 EN (JRC92618), Publications Office of the European Union, Luxembourg. https://doi.org/10.2791/675854

Bai, Y. and M. F. Cotrufo, 2022, Grassland soil carbon sequestration: Current understanding, challenges, and solutions, Science 377, 603-608. https://doi.org/10.1126/science.abo2380

Baumert, J., Heckelei, T. and H. Storm, 2024, Probabilistic crop type mapping for ex-ante modelling and spatial disaggregation, Ecological Informatics 83, 102836. https://doi.org/10.1016/j.ecoinf.2024.102836

Besnard, S., Koirala, S., Santaro, M., et al., 2021, Mapping global forest age from forest inventories, biomass and climate data, Earth System Science Data 13 4881-4896.

Bowditch, E., Santopuoli, G., Binder, F., et al., 2020, What is Climate-Smart Forestry? A definition from a multinational collaborative process focused on mountain regions of Europe. Ecosyst. Serv. 43, 101113.

Britz, W. and H. Witzke, 2014, CAPRI Model Documentation 2014, University of Bonn. http://www.capri-model.org/docs/capri_documentation.pdf

Brunet-Navarro, P., Jochheim, G., Cardellini, K., et al., 2021, Climate Mitigation by Energy and Material Substitution of Wood Products Has an Expiry Date, Journal of Cleaner Production 127026

DGAGRI, 2024a, Organic price trends, https://agridata.ec.europa.eu/extensions/DashboardPrice/OrganicPricesTrends.html

DGAGRI, 2024b, EU organic farms, https://agridata.ec.europa.eu/extensions/OrganicFarmsReport/OrganicFarmsReport.html

Doelman, J. C., Verhagen, W., Stehfest, E. and D. P. van Vuuren, 2023, The role of peatland degradation, protection and restoration for climate change mitigation in the SSP scenarios, Environmental Research: Climate 2, 035002. https://doi.org/10.1088/2752-5295/acd5f4

EEA, 2025, Greenhouse gas emissions from land use, land use change and forestry in Europe, European Environmental Agency, https://www.eea.europa.eu/en/analysis/indicators/greenhouse-gas-emissions-from-land?activeAccordion=

Eigenbrod, F., Alexander, P., Apfel, N., et al., 2026, Causal machine learning methods for understanding land use and land cover change, Landscape Ecology 41, 25. https://doi.org/10.1007/s10980-025-02279-7

Estel, S., Mader, S., Levers, C., Verburg, P. H., Baumann, M. and T. Kuemmerle, 2018, Combining satellite data and agricultural statistics to map grassland management intensity in Europe, Environmental Research Letters 13, 074020. https://doi.org/10.1088/1748-9326/aacc7a

European Commission, 2025, Good agricultural and environmental condition of land (GAEC standards), https://agriculture.ec.europa.eu/common-agricultural-policy/income-support/conditionality_en

Eurostat, 2024, Agriculture database, https://ec.europa.eu/eurostat/web/agriculture/database (accessed 13.11.2024).

FAO, 2010, "Climate-Smart" Agriculture Policies, Practices and Financing for Food Security. Adaptation and Mitigation, Rome.

FAO, 2025, Forestry production and trade database, https://www.fao.org/faostat/en/#data/FO

FAO/IIASA/ISRIC/ISS-CAS/JRC, 2012, Harmonized World Soil Database (version 1.2), FAO, Rome and IIASA, Laxenburg.

Fellmann, T., Tassinari, G., Lasarte Lopez, J., Rey Vicario, D., Beber, C., et al., 2025, Scenar 2040 - A scenario study on the Common Agricultural Policy, Publications Office of the European Union, Luxembourg, JRC142503. https://doi.org/10.2760/7381366

FiBL, 2024, Data on organic agriculture in Europe, https://statistics.fibl.org/europe.html

FRA, 2020, Global Forest Resources Assessment 2020, FAO, https://www.fao.org/documents/card/en/c/ca9825en

Fricko, O., Havlik, P., Rogelj, J., et al., 2017, The marker quantification of the Shared Socioeconomic Pathway 2: A middle-of-the-road scenario for the 21st century, Global Environmental Change 42, 251-267. https://doi.org/10.1016/j.gloenvcha.2016.06.004

Hanasaki, N., Fujimori, S., Yamamoto, T., et al., 2013, A global water scarcity assessment under Shared Socio-economic Pathways - Part 1: Water use, Hydrology and Earth System Sciences 17, 2375-2391. https://doi.org/10.5194/hess-17-2375-2013

Hiraishi, T., Krug, T., Tanabe, K., Srivastava, N., Baasansuren, J., Fukuda, M. and T. G. Troxler, 2014, 2013 Supplement to the 2006 IPCC Guidelines for National Greenhouse Gas Inventories: Wetlands, IPCC, Geneva. https://www.ipcc.ch/publication/2013-supplement-to-the-2006-ipcc-guidelines-for-national-greenhouse-gas-inventories-wetlands/

Hollmann, R., Merchant, C. J., Saunders, R., et al., 2013, The ESA Climate Change Initiative: Satellite data records for essential climate variables, Bulletin of the American Meteorological Society 94, 1541-1552. https://doi.org/10.1175/BAMS-D-11-00254.1

Humann-Guilleminot, S., Boch, S., Martinez-De Leon, G., et al., 2023, Experimental extensification of mountain grasslands restores plant species richness but not species composition in the mid-term, Journal of Applied Ecology 60, 530-540. https://doi.org/10.1111/1365-2664.14344

IIASA, 2018, Shared Socioeconomic Pathways data base version 2.0 https://tntcat.iiasa.ac.at/SspDb

IIASA, 2023, Global Biosphere Management Model (GLOBIOM) Documentation 2023, Version 1.0, International Institute for Applied Systems Analysis, Laxenburg.

IPCC, 2014, Climate Change 2014: Synthesis Report. Contribution of Working Groups I, II and III to the Fifth Assessment Report of the Intergovernmental Panel on Climate Change, IPCC, Geneva. https://www.ipcc.ch/assessment-report/ar5/

IPCC, 2019, 2019 Refinement to the 2006 IPCC Guidelines for National Greenhouse Gas Inventories, Intergovernmental Panel on Climate Change, Geneva. https://www.ipcc-nggip.iges.or.jp/public/2019rf/

Isbasoiu, A. and T. Fellmann, 2024, CAP Strategic Plans of the EU Member States - CSPs Master file and key data, Publications Office of the European Union, Luxembourg, JRC138785. https://doi.org/10.2760/3104919

Johnston, C. and V. Radeloff, 2019, Global mitigation potential of carbon stored in harvested wood products, PNAS 1904231116, www.pnas.org/cgi/doi/10.1073/pnas.1904231116

Jonsson, R., Rinaldi, F., Pilli, R., et al., 2021, Boosting the EU forest-based bioeconomy: Market, climate, and employment impacts, Technological Forecasting & Social Change, https://doi.org/10.1016/j.techfore.2020.120478

Khafagy, A. and M. Vigani, 2022, Technical change and the Common Agricultural Policy, Food Policy 109, 102267. https://doi.org/10.1016/j.foodpol.2022.102267

Kindermann, G., Obersteiner, M., Rametsteiner, E. and I. McCallum, 2006, Predicting the deforestation-trend under different carbon-prices, Carbon Balance and Management 1, 1-17.

Kindermann, G., McCallum, I., Fritz, S. and M. Obersteiner, 2008, A global forest growing stock, biomass and carbon map based on FAO statistics, Silva Fennica 42, 387-396.

Klein Goldewijk, K., Beusen, A. and P. Janssen, 2010, Long-term dynamic modeling of global population and built-up area in a spatially explicit way: HYDE 3.1, The Holocene 20, 565-573. https://doi.org/10.1177/0959683609356587

Klein Goldewijk, K., Beusen, A., Doelman, J. and E. Stehfest, 2017, Anthropogenic land use estimates for the Holocene - HYDE 3.2, Earth System Science Data 9, 927-953. https://doi.org/10.5194/essd-9-927-2017

Kremmydas, D., Ciaian, P. and E. Baldoni, 2023, Modelling conversion to organic agriculture with an EU-wide farm model, Bio-Based and Applied Economics 12, 261-304.

Krisztin, T., Piribauer, P., & Wögerer, M. (2022). A spatial multinomial logit model for analysing urban expansion. *Spatial Economic Analysis*, *17*(2), 223–244. https://doi.org/10.1080/17421772.2021.1933579

Lesiv, M., Schepaschenko, D., Buchhorn, M., et al., 2022, Global forest management data for 2015 at a 100 m resolution, Scientific Data 9, 199. https://doi.org/10.1038/s41597-022-01332-3

Leskinen, P., Cardellini, G., González-García, S., et al., 2018, Substitution effects of wood-based products in climate change mitigation, From Science to Policy 7. European Forest Institute. https://doi.org/10.36333/fs07

Martin, N. and J. Couwenberg, 2021, Organic soils in national inventory submissions of EU countries, Proceedings of the Greifswald Mire Centre. https://www.greifswaldmoor.de/files/dokumente/GMC%20Schriften/2021_Martin&Couwenberg.pdf

McFadden, D., 1974, Conditional logit analysis of qualitative choice behavior, in: P. Zarembka (ed.), Frontiers in Econometrics, Academic Press, New York, 105-142.

Myllyviita, T., Soimakallio, S., Judl, J. and J. Seppälä, 2021, Wood substitution potential in greenhouse gas emission reduction–review on current state and application of displacement factors, Forest Ecosystems 8:42 https://doi.org/10.1186/s40663-021-00326-8

Nabuurs, G., Delacote, P., Ellison, D., Hanewinkel, M., Hetemäki, L., Lindner, M., Ollikainen, M., 2017, By 2050 the mitigation effects of EU forests could nearly double through climate smart forestry. Forests 8, 1–14. https://doi.org/10.3390/f8120484.

Nabuurs, G., Verkerk, H., Schelhaas, M., Ramon, J., Trasobares, A., Cienciala, E., 2018, Climate-Smart Forestry : quantification of mitigation impacts in three case regions in Europe Outline – Concept of Climate-Smart Forestry – Three cases regions in Europe. Brussels.

Niemi, J., Soimakallio, S. and E. Hurmekoski, 2025, Carbon credits through wood use: revisiting the maximum potential and sensitivity to key assumptions, GCB Bioenergy 17, 70017. https://doi.org/10.1111/gcbb.70017

OECD/FAO, 2023, OECD-FAO Agricultural Outlook 2023-2032, OECD Publishing, Paris. https://doi.org/10.1787/08801ab7-en

O'Neill, B. C., Carter, T. R., Ebi, K., et al., 2020, Achievements and needs for the climate change scenario framework, Nature Climate Change 10, 1074-1084. https://doi.org/10.1038/s41558-020-00952-0

Packalen, T., Sallnäs, O., Sirkiä, S., Korhonen, K. T., Salminen, O., Vidal, C., et al., 2014, The European forestry dynamics model: concept, design and results of first case studies, EUR - Scientific and Technical Research Reports. https://doi.org/10.2788/153990

Petersson, H., Ellison, D., Mensah, A., et al.,2022, On the role of forests and the forest sector for climate change mitigation in Sweden, GCB-Bioenergy 14, 793-813. DOI:10.1111/gcbb.12943

Pignotti, D., Stepanyan, D., Curtiss, J., Neuenfeldt, S., Lampkin, N. and A. Gocht, 2026, NUTS 2-level data for organic and conventional agricultural activities in the European Union (2010-2020), Zenodo [Dataset]. https://doi.org/10.5281/zenodo.18470509

Riahi, K., van Vuuren, D. P., Kriegler, E., et al., 2017, The Shared Socioeconomic Pathways and their energy, land use, and greenhouse gas emissions implications: An overview, Global Environmental Change 42, 153-168. https://doi.org/10.1016/j.gloenvcha.2016.05.009

Rodriguez-Rigueiro, F. J., Santiago-Freijanes, J. J., Mosquera-Losada, M. R., et al., 2021, Silvopasture policy promotion in European Mediterranean areas, PLoS ONE 16, e0245846. https://doi.org/10.1371/journal.pone.0245846

Schelhaas, M. J., Eggers, J., Lindner, M., Nabuurs, G. J., Pussinen, A., Päivinen, R., et al., 2007, Model documentation for the European Forest Information Scenario model (EFISCEN), Alterra, Wageningen. https://edepot.wur.nl/31239

Schiavina, M., Melchiorri, M., Pesaresi, M., et al., 2023, GHSL Data Package 2023, Publications Office of the European Union, Luxembourg, JRC133256. https://doi.org/10.2760/098587

Schievano, A., Perez-Soba, M., Bosco, S., et al., 2023, JRC-Farming-Practices dataset (version 2023) - An evidence library of the effects of farming practices on the environment and the climate, European Commission, Joint Research Centre [Dataset]. https://doi.org/10.2905/4e3c371a-be72-4ea0-aa0b-45f8cdda2064

Schils, R. L. M., Bufe, C., Rhymer, C. M., et al., 2022, Permanent grasslands in Europe: Land use change and intensification decrease their multifunctionality, Agriculture, Ecosystems & Environment 330, 107891. https://doi.org/10.1016/j.agee.2022.107891

Schreiner, F.-R., Holzel, N., Hamer, U., et al., 2026, Slow and context-dependent: Responses to grassland extensification across a comprehensive set of ecosystem attributes, Agriculture, Ecosystems & Environment 401, 110277. https://doi.org/10.1016/j.agee.2026.110277

Skalský, R., Tarasovičová, Z., Balkovič, J., Schmid, E., Fuchs, M., Moltchanova, E., Kindermann, G. and P. Scholtz, 2008, GEO-BENE global database for bio-physical modelling v. 1.0: concepts, methodologies and data, International Institute for Applied Systems Analysis, Laxenburg.

Soimakallio, S., Böttcher, H., Niemi, J., et al., 2022, Closing an open balance: The impact of increased tree harvest on forest carbon. GCB Bioenergy, 14, 989–1000. https://doi.org/10.1111/gcbb.12981

Stoorvogel, J. J., 2014, S-World: A global map of soil properties for modelling, in: GlobalSoilMap: Basis of the global spatial soil information system, 227-231.

Tegetmeyer, C., Kaiser, M. and A. Barthelmes, 2025, The European Wetland Map ('EWM') (v3), Zenodo [Dataset]. https://doi.org/10.5281/zenodo.14745285

van den Pol-van Dasselaar, A., Bastiaansen-Aantjes, L., Bogue, F., O'Donovan, M. and C. Huyghe (eds.), 2019, Grassland use in Europe: A syllabus for young farmers, Editions Quae, Versailles.

van Huijstee, J., van Bemmel, B., Bouwman, A. and F. van Rijn, 2018, Towards an urban preview: Modelling future urban growth with 2UP, PBL Netherlands Environmental Assessment Agency, The Hague, PBL publication number 3255.

Verkerk, P., Costanza, R., Hetemäki, L., et al., 2020, Climate-smart forestry: the missing link. For Policy Econ. https://doi.org/10.1016/j.forpol.2020.102164.

Wilson, D., Blain, D., Couwenberg, J., Evans, C. D., Murdiyarso, D., Page, S. E., et al., 2016, Greenhouse gas emission factors associated with rewetting of organic soils, Mires and Peat 17. https://doi.org/10.19189/MaP.2016.OMB.222

Winkler, K., Fuchs, R., Rounsevell, M. and M. Herold, 2021, Global land use changes are four times greater than previously estimated, Nature Communications 12, 2501. https://doi.org/10.1038/s41467-021-22702-2

Zhao, J., Wei, X. and L. Li, 2022, The potential for storing carbon by harvested wood products. Frontiers in Forests and Global Change, 5:1055410. DOI:10.3389/ffgc.2022.1055410

8. Annexes

8.1. ANNEX LAND SUPPLY ELASTICITIES

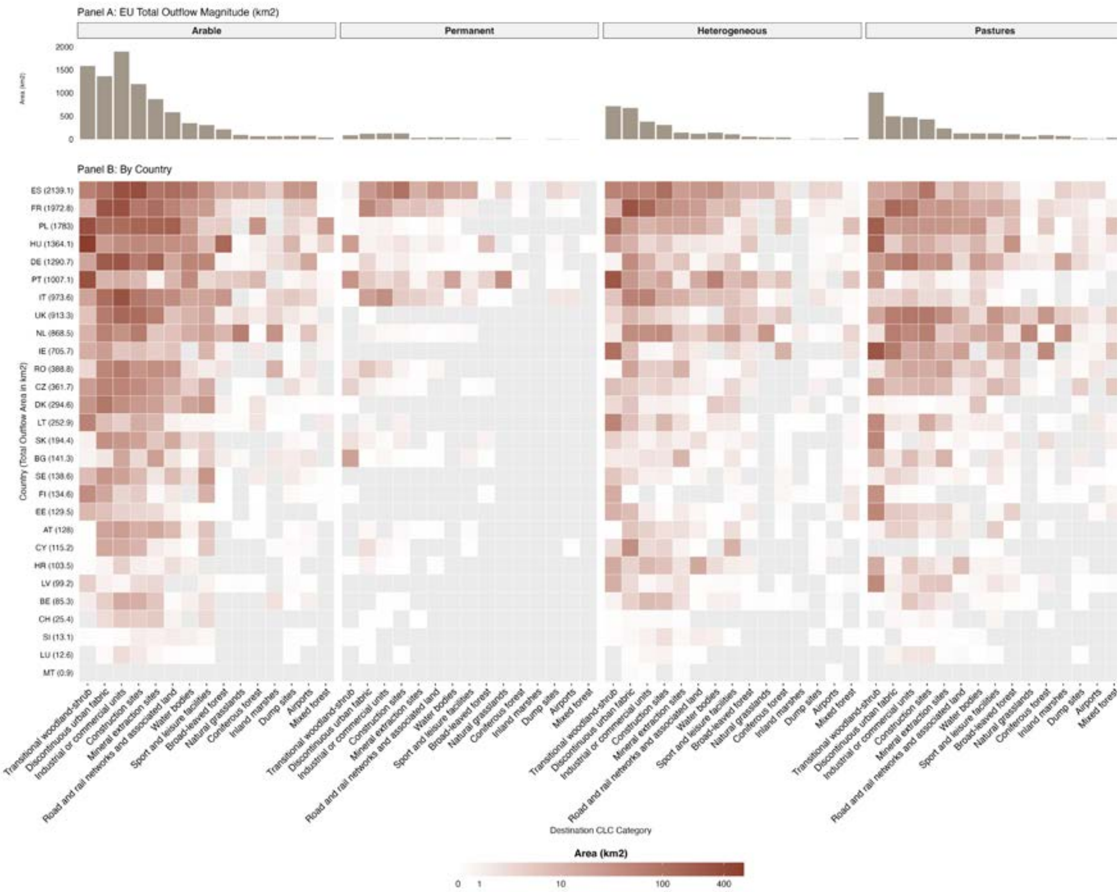

Figure 16: Empirically observed land-cover transitions from agricultural use across the EU (2000–2018).

Note: Panel A displays the total EU-wide magnitude of land outflows (in km²) into four primary agricultural classes from non-agricultural CORINE Land Cover (CLC) categories. Panel B provides a country-level breakdown of these outflows via a heatmap, highlighting the pronounced spatial heterogeneity of agricultural expansion sources.

8.2. ANNEX LUM GEODATABASE – IMAGE/MAGNET MAPPING

Table 12: Mapping of LUM database and IMAGE/MAGNET land-use/cover categories

CODE	LUM DATABASE CATEGORY	IMAGE/MAGNET LAND-USE/COVER MAPPING
1	Primary forest	natural forest
2	Close-to-nature management	natural forest

CODE	LUM DATABASE CATEGORY	IMAGE/MAGNET LAND-USE/COVER MAPPING
3	Combined objective forestry	managed forest
4	Intensive forestry	managed forest
5	Very intensive forestry	managed forest
6	Irrigated arable cropland	cropland
7	Rainfed intensive arable cropland	cropland
8	Rainfed extensive arable cropland	cropland
9	Irrigated permanent cropland	cropland
10	Rainfed intensive permanent cropland	cropland
11	Rainfed extensive permanent cropland	cropland
14	Agroforestry	cropland
15	Very high density managed pasture system	managed grazing land
16	High density managed pasture system	managed grazing land
17	Moderate density managed pasture system	managed grazing land
18	Low density managed pasture system	managed grazing land
19	Very high density managed grassland	managed grazing land
20	High density managed grassland	managed grazing land
21	Moderate density managed grassland	managed grazing land
22	Low density managed grassland	managed grazing land
23	Rough grazing	managed grazing land
24	Silvo-pastoral agroforestry	managed grazing land
25	Managed semi-natural and natural grassland	managed grazing land
26	Unmanaged semi-natural and natural grassland	other natural land
27	High intensity urban (buildings)	built-up area
28	Medium intensity urban (buildings)	built-up area
29	Low intensity urban (buildings)	built-up area
30	Infrastructure	built-up area
31	Other urban	built-up area
321	3.2.1 Natural grasslands	other natural land
322	3.2.2 Moors and heathland	other natural land
323	3.2.3 Sclerophyllous vegetation	other natural land
324	3.2.4 Transitional woodland-shrub	other natural land
331	3.3.1 Beaches, dunes, sands	other natural land
332	3.3.2 Bare rocks	other natural land
333	3.3.3 Sparsely vegetated areas	other natural land
334	3.3.4 Burnt areas	other natural land
335	3.3.5 Glaciers and perpetual snow	ice
411	4.1.1 Inland marshes	other natural land
412	4.1.2 Peat bogs	other natural land

CODE	LUM DATABASE CATEGORY	IMAGE/MAGNET LAND-USE/COVER MAPPING
421	4.2.1 Salt marshes	other natural land
422	4.2.2 Salines	other natural land
423	4.2.3 Intertidal flats	other natural land
511	5.1.1 Water courses	other natural land
512	5.1.2 Water bodies	other natural land
521	5.2.1 Coastal lagoons	other natural land
522	5.2.2 Estuaries	other natural land
523	5.2.3 Sea and ocean	other natural land
2012	Intensive heterogeneous arable classes	cropland
2013	Extensive heterogeneous arable classes	cropland
3012	Intensive heterogeneous permanent classes	cropland
3013	Extensive heterogeneous permanent classes	cropland
4012	Intensive heterogeneous grassland classes	managed grazing land
4013	Extensive heterogeneous grassland classes	managed grazing land
10000	Leftover forest	natural forest
20000	Leftover cropland	other anthropogenic land
40000	Leftover grassland	other anthropogenic land